For the special issue honoring Professor Roy Jackson

Optimization Framework for the Synthesis of Chemical Reactor Networks

C. A. Schweiger and C. A. Floudas *
Department of Chemical Engineering,
Princeton University,
Princeton, NJ 08544-5263, USA

Abstract–The reactor network synthesis problem involves determining the type, size, and interconnections of the reactor units, optimal concentration and temperature profiles, and the heat load requirements of the process. A general framework is presented for the synthesis of optimal chemical reactor networks via an optimization approach. The possible design alternatives are represented via a process superstructure which includes continuous stirred tank reactors and cross flow reactors along with mixers and splitters that connect the units. The superstructure is mathematically modeled using differential and algebraic constraints and the resulting problem is formulated as an optimal control problem. The solution methodology for addressing the optimal control formulation involves the application of a control parameterization approach where the selected control variables are discretized in terms of time invariant parameters. The dynamic system is decoupled from the optimization and solved as a function of the time invariant parameters. The algorithmic framework is implemented in the optimization package MINOPT which is used as a tool for solving the reactor network synthesis problem. The proposed approach is applicable to general problem formulations and its utility is illustrated through the application to numerous examples including both constant and variable density problems, isothermal and nonisothermal operation, as well as complex reaction mechanisms with the kinetic and thermodynamic data provided by Chemkin.

1 Introduction

The overall process synthesis problem deals with determining the entire process flowsheet which converts the given raw materials into the desired products. It includes aspects of the process such as reaction, separation, recycle, and energy integration. Rigorous mathematical approaches to process synthesis are capable of determining the interactions among the various parts of the process as discussed in Floudas[1]. Many of the process synthesis approaches have addressed process subsystems such as heat exchanger networks, separation systems, and reactor network synthesis. The reaction step is often the heart of a chemical process and the foundation for the process design. The reaction chemistry determines the character of

*Author to whom all correspondence should be addressed.

the entire process and has a significant impact on the design of the overall process. Although only part of the overall synthesis problem, a carefully designed reactor network is crucial to the design of the entire process.

An extensive review of reactor network synthesis approaches can be found in Hildebrandt and Biegler[2]. The focus of the previous work has been on manipulating flow patterns and mixing patterns within the reactors. The Plug Flow Reactor (PFR) and the Continuous Stirred Tank Reactor (CSTR) have long been recognized as two extreme ideal cases where the PFR models no mixing and the CSTR models perfect mixing. Different approaches have been proposed to develop models which capture the mixing aspects between these two extremes. Other methods have been proposed which incorporate the different reactor models into reactor network synthesis problem.

Some of the early work in reactor optimization focused on analyzing the effects of different mixing models. In the work of Dyson and Horn[3], a tubular reactor is designed for an exothermic reaction where the temperature is controlled by distributing the cold feed along the reactor. In the work of Horn and Tsai[4], the effects of local and global mixing were investigated on tubular reactors involving recycle or bypass streams. The problem is solved as an optimal control problem using adjoint methods. One of the earliest works which addressed the idea of a reactor network was that of Jackson[5]. A network of parallel plug flow reactors interconnected with sidestreams was postulated. The model involved source points and sink points along the tubular reactors to allow for manipulation of the mixing pattern. This work was extended to include local mixing by Ravimohan[6] by incorporating CSTRs into the network along with a discrete decision. An axial dispersion model was developed by Paynter and Haskins[7] which avoids the discrete decisions on the reactor types. The problem was formulated as an optimal control problem where the decision variable was the dispersion coefficient. The value of the dispersion coefficient could vary continuously from one limit (CSTR) to the other (PFR). The ideas of Jackson[5] were further extended by Achenie and Biegler[8] by using an axial dispersion reactor instead of the PFR as the fundamental unit in the network. The model allowed for series and parallel combinations and allowed for more general situations than those where only PFRs are considered. The problem was formulated as an optimal control problem and solved by coupling the solution of a two point boundary value problem with a successive quadratic programming approach. The work of Achenie and Biegler[9] continued along the same lines by using a recycle reactor unit as the fundamental unit in the network superstructure. This simplified the problem and reduced the computational effort, but the model was less general.

A reactor network superstructure which included CSTRs and PFRs with various interconnections was formulated by Kokossis and Floudas[10;11;12]. In the problem formulation, the PFRs were approximated by a series of equal sized sub-CSTRs to eliminate the differential equations, and integer variables were used to represent the existence of reactor units. This resulted in a large-scale MINLP formulation that was solved using Generalized Benders Decomposition along with an initialization strategy. The approach was capable of handling arbitrary kinetics for both isothermal and nonisothermal situations. Stability constraints were incorporated in to the synthesis problem to avoid the selection of unstable networks[13]. The approach allowed for general network configurations, but led to large, complex, nonconvex MINLP formulations that exhibit multiple local solutions.

The key advantage of the superstructure-based approaches is that they can determine

simultaneously the objective value and the explicit optimal reactor network configuration and operating conditions. One of the limitations of the superstructure based approaches is that the optimal solution is only as rich as the initial superstructure. The true optimal reactor network can not be found if it is not contained within the superstructure. However, increasing the richness of the superstructure comes at the cost of increasing the size and complexity of the model. In addition, the model formulations for these problems are nonlinear and nonconvex and the solution procedures relied on local optimization.

In order to address the limitations involved with the superstructure based approaches, a performance index free of the limitations imposed by the reactor types and configuration was deemed necessary. These methods were proposed to determine a target or bound on the performance index of the reactor network regardless of the reactor types and configuration. These methods expanded on the early work of Horn[14] which defined the attainable region as the set of all possible conditions that can be achieved through reaction and mixing. In the work of Glasser et al.[15], the geometric properties of the attainable region were developed along with a geometric approach for defining the attainable region in the space of the variables needed to define the objective function. The attainable region concepts were further developed by Hildebrandt et al.[16] where the properties were applied to systems with nonconstant densities and heat capacities. In Hildebrandt and Glasser[17] the concepts were extended to three dimensional examples. These targeting methods were shown to be powerful in terms of the information they provided, but they relied on geometric techniques that were difficult to apply to higher dimensions.

In the work of Achenie and Biegler[18], a target was developed based on the residence time distribution function (RTD). Both macro and micro mixing concepts were incorporated by considering maximum mixed and segregated environments. The problem was formulated as a nonlinear program which avoided the dimensionality problems of geometric or graphical approaches. Since the reactor network was not automatically determined, the reactor network suggested by the RTD was developed after the RTD was determined. This approach was further developed by Balakrishna and Biegler[19;20] where feasible regions for the optimization were successively generated in an iterative procedure. Two approaches were proposed for expanding the feasible region: a constructive approach where convex regions were extended recursively and a multi-compartment approach where additional compartments are added at each stage. This constructive approach ensured that only the simplest model required was solved. The solutions were given in terms of the RTD and the reactor network was not directly determined. With the targeting approach now posed as an optimization problem, various approaches were described in Balakrishna and Biegler[21]. Applications to isothermal and nonisothermal systems, energy integration, and simultaneous reaction, separation, and energy systems were considered. The work of Lakshmanan and Biegler[22] combined the ideas of the targeting approaches with the superstructure approaches. Reactor modules consisting of CSTRs and Differential Sidestream Reactors (DSRs) were considered as the fundamental building blocks of the superstructure. The properties of the attainable region were applied to ensure that a sufficiently rich superstructure is proposed. The resulting model was an MINLP which was solved sequentially in a constructive manner to ensure that simple models were solved and that simple networks were determined.

Recently, an important set of the fundamental properties of the attainable region which can be used as guidelines in the design of reactor systems were presented in Feinberg and

Hildebrandt[23]. Several key properties of the attainable region were outlined and the effect that reactor types have on the shape of the attainable region was described. The extreme points of the attainable region were shown to be accessible by simple combinations of elementary reactor types. The analysis showed that PFR trajectories access almost all of the attainable region while the CSTRs and sidestream reactors connect the PFR sections of the attainable region.

This work focuses on addressing two disadvantages of the superstructure based approach: the large, complex formulations and the approximation to the PFR. By modeling the PFR with differential and algebraic equations and incorporating differential sidestreams to achieve Maximum Mixed and Segregated Flow reactors, a simpler model which preserves the richness of the MINLP formulation is generated. Another issue addressed in the development of this synthesis approach is that the proposed method must be capable of being directly incorporated into a full process synthesis approach.

In Section 2 the reactor network synthesis problem is defined and the optimization approach to solving this synthesis problem is described. The process superstructure is given and the mathematical models which describe the superstructure are given. In Section 3 the problem is formulated as an optimal control problem and a solution algorithm is proposed. In Section 4 the algorithmic framework is described and in Section 5 extensive computational studies that illustrate the features of the proposed approach are presented along with comparisons to other approaches.

2 Reactor Network Synthesis

In reactor network synthesis, the goal is to determine the reactor network that transforms the given raw materials into the desired products. The following information is assumed to be given in the problem definition:

- the reaction mechanism
- the kinetic data
- the enthalpic data
- the inlet stream(s) data
- the performance objective (output).

The synthesis problem is to determine:

- the type, size, and interconnection of reactor units
- the stream flowrates, compositions, and temperatures
- the composition and temperature profiles
- the heating and cooling requirements

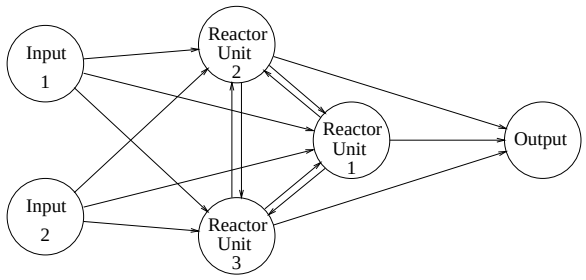

Figure 1: Conceptual Reactor Network Superstructure.

The optimization approach to process synthesis is applied to the reactor synthesis problem. This approach involves three steps: (i) the representation of process design alternatives of interest through a process superstructure, (ii) the mathematical modeling of the superstructure, and (iii) the development of a solution procedure to extract the optimal process flowsheet from the superstructure. The key feature of this approach is the postulation of a superstructure which contains all possible structural alternatives. The superstructure must be sufficiently rich to contain all possible network configurations, as well as simple enough to eliminate redundancies and reduce complexity. A well-developed superstructure facilitates in the modeling and solution of the process synthesis problem.

2.1 Reactor Network Superstructure

The superstructure, as described by Floudas[1], is developed based on elementary graph theory ideas. The general superstructure includes nodes to represent the units, inputs, and outputs of the process and arcs to represent the flow of material between the nodes. One-way arcs represent connections from the inputs to the units and from the units to the outputs while two-way arcs represent interconnections between process units. The result is a bipartite planar graph which represents all of the options of the superstructure. A conceptual reactor network superstructure is shown in Figure 1 where the the nodes correspond to the reactors, mixers, and splitters.

One of the key issues in the superstructure based approach for reactor network synthesis is determining which reactors should be in the superstructure. The richness of the superstructure is determined by the variety and number of reactor units included and the interconnections among them. However, too many reactors and reactor types can unnecessarily complicate the superstructure and give rise to redundancies. The work of Feinberg and Hildebrandt[23] showed that the only reactor types required to access all possible compositions for a given reaction mechanism are the fundamental reactor types of the PFR, CSTR, and differential sidestream reactors. Thus, the design of a reactor network is more a question of how to incorporate the traditional reactors and less of a speculation about alternative devices.

For the reason above, the following different types of reactor units are considered:

- Continuous Stirred Tank Reactor (CSTR)
- Plug Flow Reactor (PFR)

- Maximum Mixed Reactor (MMR)
- Segregated Flow Reactor (SFR)
- Cross Flow Reactor (CFR)

The CSTR is assumed to be perfectly mixed such that there are no spatial variations in concentration, temperature, and reaction rate. The PFR is a tubular reactor where there are no radial variations in concentration, temperature and reaction rate. The MMR, SFR, and CFR are different types of differential sidestream reactors. The MMR allows for mixing at the earliest possible moment by utilizing a side feed along a tubular reactor while the SFR allows for mixing at the latest possible moment by using a side exit stream. The CFR employs both the side feed and side exit streams. Schematic models of all the reactors are shown in Figure 2. The CFR can be viewed as a generalization of the PFR, MMR, and SFR since it incorporates the aspects of each into a single unit. Therefore, only the CSTR and CFR need to be in the superstructure since the PFR, MMR, and SFR can be obtained from the CFR.

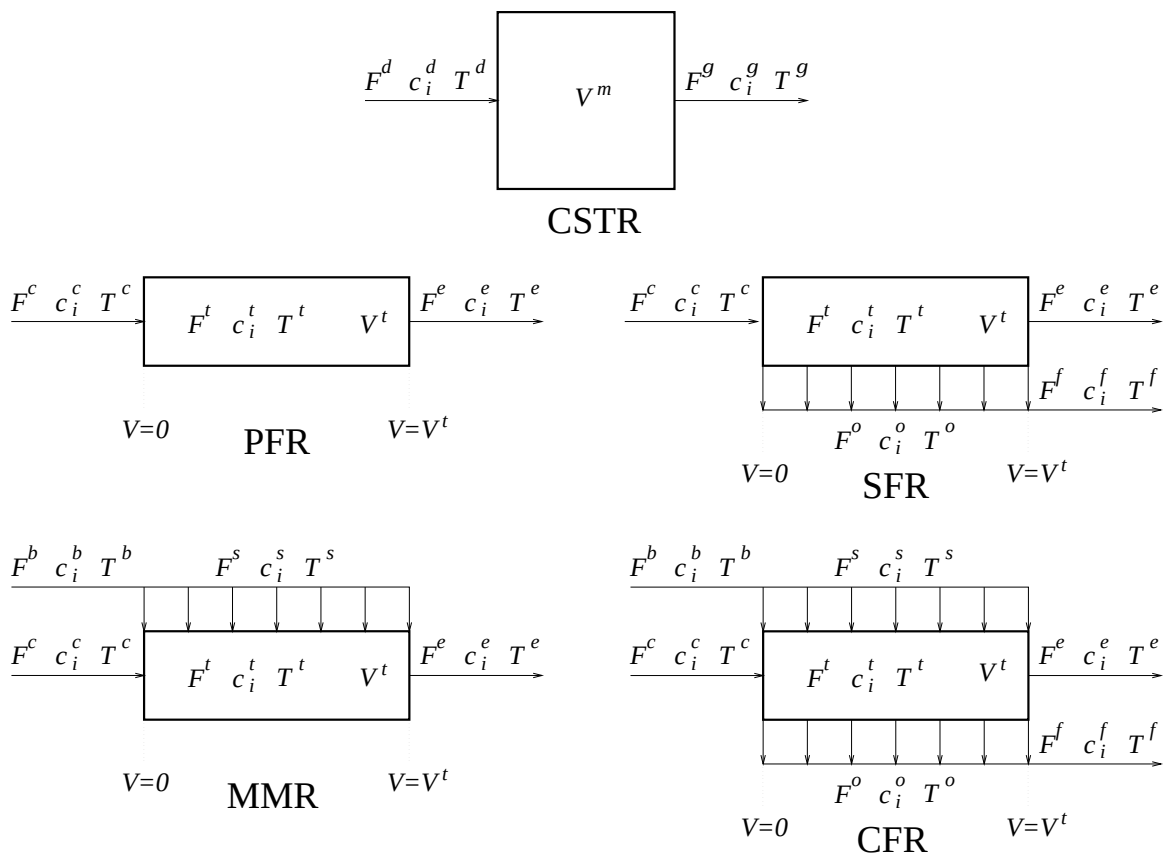

Figure 2: Schematic representation of the various reactor units.

These units are incorporated into the superstructure along with mixers and splitters that interconnect the various units to create the reactor network. These allow for various flow

patterns through the network such as parallel or series combinations. An example of such a superstructure that consists of a CSTR and a CFR is shown in Figure 3.

2.2 Mathematical Modeling of Superstructure

Once the superstructure has been established, the next step in the optimization approach is its mathematical modeling. The model formulation involves material and energy balances around all of the units in the superstructure: the feed splitter, the mixers before the reactor units, the reactor units (shown in Figure 2), the splitters after the reactor units, and the product mixer.

The objective function for the reactor network synthesis problem can have a number of different forms. One objective is to maximize the yield of a desired product. Another objective may be based upon economic criteria reflected by the value of the product, the cost of the reactors, and the cost of the utilities. The constraints for the problem consist of material and energy balances for the units in the process and logical constraints for maintaining acceptable arrangement of process units.

The mathematical modeling of the mixers, splitters, and CSTRs leads to algebraic equations while the modeling of the PFR, MMR, SFR and CFR leads to differential equations. The overall mathematical model for the superstructure is a system of Differential and Algebraic Equations (DAEs). The variables in the model are the flowrates, compositions, temperatures, reactor volumes, and enthalpies.

The superstructure has been developed for general situations and likewise the modeling of the superstructure can be applied to general situations. No assumptions such as constant density or ideal gas need to be made; however, information is required for closure relationships so that the model can be fully specified. For example, when reaction rates are given as functions of concentration, a relationship which determines the concentration of a species based on the composition and flowrate of the stream must be known. General reaction modeling and general reaction kinetics are permissible in the model. The stoichiometry of the set of reactions is assumed to be known and the set of stoichiometrically independent reactions is given. The reactions are conveniently described by the matrix, $\nu_{i,j}$, where the elements represent the stoichiometric coefficients of species i in reaction j. (The index i is used to denote a component in the set of components I and j is used to represent a reaction in the set of reactions J.)

The rate of reaction, r_j, is defined as the amount of reaction per unit time per unit volume of mixture. In general, the reaction rate depends on the concentration of the species, c_i, and the temperature, T, and is expressed as:

$$r_j = f_j^r(c_i, T)$$

The rate expressions for the reactions may take on a variety of forms such as power laws or Langmuir-Hinshelwood type expressions. The temperature dependence is usually described by the Arrhenius law. The rate of production or consumption of the species is given by the product of $\nu_{i,j}$ and r_j.

For the modeling of the superstructure, the variables used are the volumetric flowrates, F, the molar concentrations, c_i, molar density, ρ, and the molar enthalpies, H_i. Superscripts are

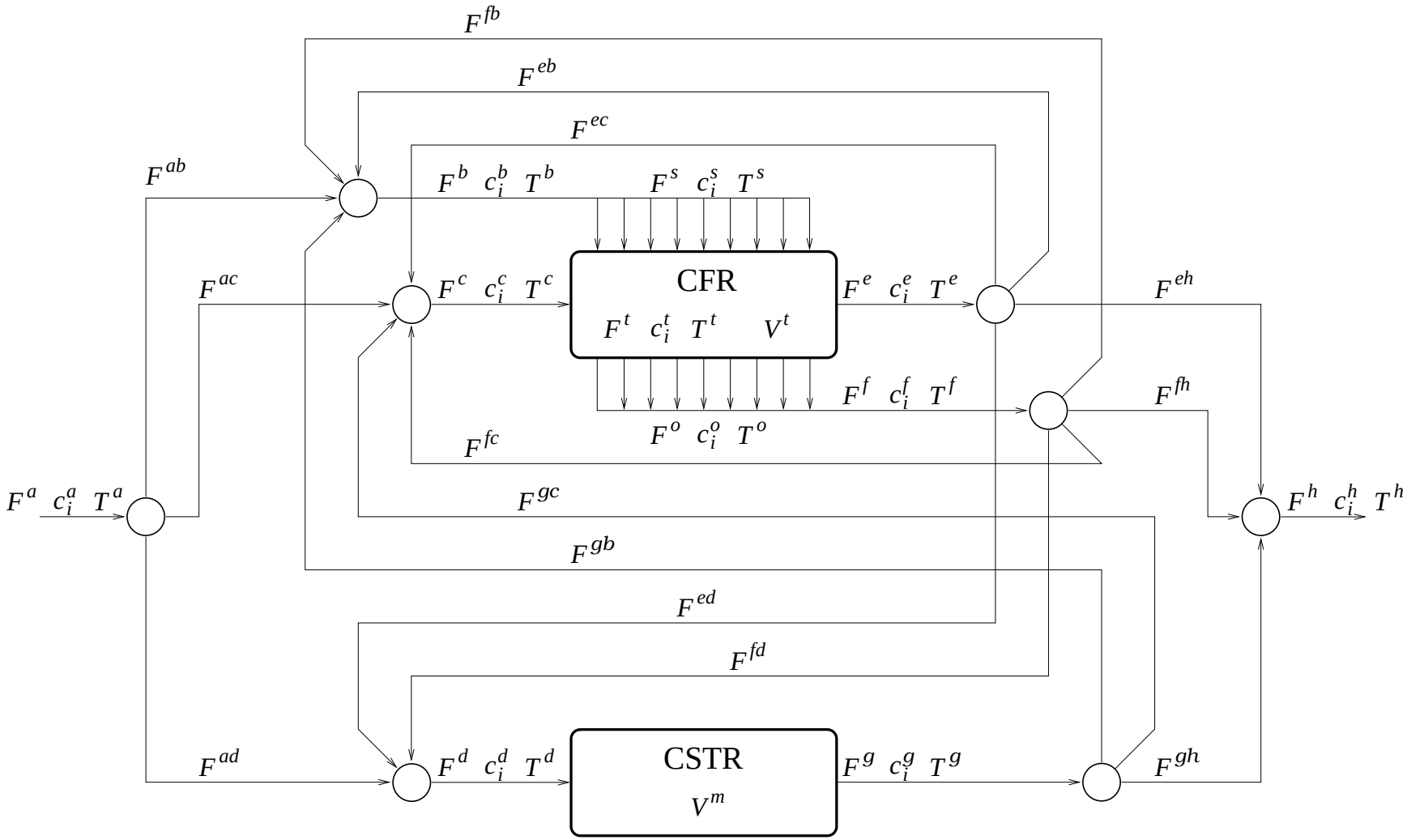

Figure 3: Example of a reactor network superstructure.

Table 1: Superscript notation for the reactor network superstructure.

Superscript	Stream
a	feed stream
b	CFR side inlet stream
c	CFR main inlet stream
d	CSTR inlet stream
e	CFR main outlet stream
f	CFR side outlet stream
g	CSTR outlet stream
h	product stream
m	CSTR
s	CFR side entering stream
t	CFR
o	CFR side leaving stream

used to identify which variables correspond to which streams or units, and subscripts are used to index the variables for multiple occurrences. The superscripts and their corresponding identifications are listed in Table 1 and the subscripts and their corresponding sets are listed in Table 2. A double superscript and double subscript are used to denote a connecting streams from one unit to another. For example, the flowrate $F^{ac}_{r,k}$ is the volumetric flowrate from feed splitter r to the kth CFR main feed, and $c^{a}_{r,i}$ is the concentration of component i in feed stream r.

2.2.1 CSTR

The material balance for the CSTR units takes the form:

$$c^{g}_{l,i}F^{g}_{l} - c^{d}_{l,i}F^{d}_{l} = V^{m}_{l}\sum_{j\in J}\nu_{i,j}r^{m}_{l,j} \quad \forall i \in I \quad \forall l \in L \tag{1}$$

where $c^{d}_{l,i}$ and $c^{g}_{l,i}$ are the molar concentrations of component i into and out of reactor l respectively; F^{g}_{l} and F^{d}_{l} are the volumetric flowrates out of and into reactor l; $\nu_{i,j}$ is the stoichiometric matrix for the reactions, and $r^{m}_{l,j}$ is the rate of reaction j in reactor l.

The energy balance is

$$H^{g}_{l}\rho^{g}_{l}F^{g}_{l} - H^{d}_{l}\rho^{d}_{l}F^{d}_{l} = Q^{m}_{l} \quad \forall i \in I \quad \forall l \in L \tag{2}$$

where H^{d}_{l} and H^{g}_{l} are the total molar enthalpies in the inlet and outlet streams respectively, ρ^{d}_{l} and ρ^{g}_{l} are the molar densities of the inlet and outlet streams, and Q^{m}_{l} is the heat flow into the reactor.

2.2.2 CFR

For the modeling of the CFR, the following assumptions are made:

Table 2: Subscript notation for the reactor network superstructure.

Subscript	Set	Correspondence
i	I	Components
j	J	Reactions
k	K	CFRs
l	L	CSTRs
r	R	Feeds
p	P	Products

- steady one-dimensional flow
- the influx (sidestream) is instantaneously mixed with the reactants in the reactor
- no axial diffusion

A differential element of the CFR as shown in Figure 4 is used for the material and energy balances. The CFR is mathematically modeled by differential equations over the volume of the reactor. The reactor model has differential sidestreams both entering and exiting along the length of the reactor, as well as differential heating and cooling along the reactor.

The material balance is

$$\frac{d(c^t_{k,i}F^t_k)}{dV} = c^s_{k,i}\frac{d\bar{F}^s_k}{dV} - c^t_{k,i}\frac{d\bar{F}^o_k}{dV} + \sum_{j\in J}\nu_{i,j}r^t_{k,j} \quad \forall i \in I \quad \forall k \in K \tag{3}$$

where $c^t_{k,i}$ is the molar concentration of species i within reactor, $c^s_{k,i}$ is the molar concentration of species i in the feed sidestream to reactor k, and F^t_k is the volumetric flowrate in reactor k. The differentials $\frac{d\bar{F}^s_k}{dV}$ and $\frac{d\bar{F}^s_k}{dV}$ are the differential flows from the feed sidestream and to the exit sidestream. As before, $\nu_{i,j}$ is the stoichiometric matrix and $r^t_{k,j}$ is the reaction rate vector. The independent variable for the differential equation is the volume of the reactor, V.

The energy balance is

$$\frac{d(H^t_k\rho^t_kF^t_k)}{dV} = H^s_k\rho^s_k\frac{d\bar{F}^s_k}{dV} - H^t_k\rho^t_k\frac{d\bar{F}^o_k}{dV} + \frac{dQ^t_k}{dV} \quad \forall k \in K \tag{4}$$

where H^t_k and ρ^t_k are the molar enthalpy and molar density within reactor k, H^s_k and ρ^s_k are the enthalpy and density of the side feed stream, and $\frac{dQ^t_k}{dV}$ is the differential heat flow rate into reactor k.

The initial conditions for the differential equations are the feed conditions of the reactor:

$$c^t_{k,i}\big|_{V=0} = c^c_{k,i} \quad \forall i \in I \quad \forall k \in K \tag{5}$$

$$F^t_k\big|_{V=0} = F^c_k \quad \forall k \in K \tag{6}$$

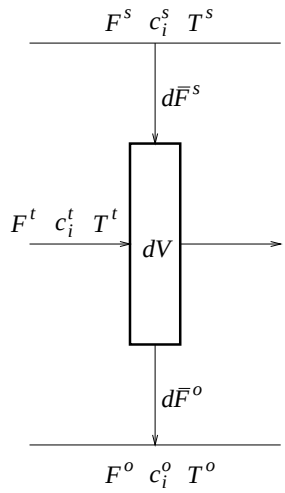

Figure 4: Differential element of the CFR.

$$H_k^t\big|_{V=0} = H_k^c \quad \forall k \in K \tag{7}$$

The final conditions of the CFR are connected to the outlet of the CFR through constraints imposed when $V = V^t$.

$$c_{k,i}^t\big|_{V=V^t} = c_{k,i}^e \quad \forall i \in I \quad \forall k \in K \tag{8}$$

$$F_k^t\big|_{V=V^t} = F_k^e \quad \forall k \in K \tag{9}$$

$$H_k^t\big|_{V=V^t} = H_k^e \quad \forall k \in K \tag{10}$$

The material balance for the feed sidestream is

$$\frac{d(c_{k,i}^s F_k^s)}{dV} = -c_{k,i}^s \frac{d\bar{F}_k^s}{dV} \quad \forall i \in I \quad \forall k \in K \tag{11}$$

and the energy balance is

$$\frac{d(H_k^s \rho_k^s F_k^s)}{dV} = H_k^s \rho_k^s \frac{d\bar{F}_k^s}{dV} \quad \forall k \in K \tag{12}$$

The values of $c_{k,i}^s$, H_k^s, and ρ_k^s as functions of the reactor position must be known. The equations can be simplified by assuming the conditions of the sidestream do not change along the length of the reactor. If the conditions are constant in V, the material and energy balances both simplify to

$$\frac{dF_k^s}{dV} = -\frac{d\bar{F}_k^s}{dV} \quad \forall k \in K \tag{13}$$

The sidestream formed from the material leaving the reactor is described by the following differential equation:

$$\frac{d(c^o_{k,i}F^o_k)}{dV} = c^t_{k,i}\frac{d\bar{F}^o_k}{dV} \quad \forall i \in I \quad \forall k \in K \tag{14}$$

where $c^o_{k,i}$ and F^o_k are the molar concentration and volumetric flowrate of the side exit stream and $\frac{d\bar{F}^o_k}{dV}$ is the differential flow from the reactor. The energy balance is

$$\frac{d(H^o_k\rho^o_kF^o_k)}{dV} = H^t_k\rho^t_k\frac{d\bar{F}^o_k}{dV} \quad \forall k \in K \tag{15}$$

The final conditions of the side exit stream are connected to the side exit outlet stream through the following constraints:

$$c^o_{k,i}\big|_{V=V^t} = c^f_{k,i} \quad \forall i \in I \quad \forall k \in K \tag{16}$$

$$F^o_k|_{V=V^t} = F^f_k \quad \forall k \in K \tag{17}$$

$$H^o_k|_{V=V^t} = H^f_k \quad \forall k \in K \tag{18}$$

A key characteristic of the CFR modeling that should be noted is that the differential equations have variable initial conditions. Since the initial conditions correspond to the inlet conditions for the reactor, they must be optimized in the solution procedure.

2.2.3 Splitters

Splitters are situated in the superstructure to split the feed for each of the reactor units and to split the output from each of the reactors for feed to the rest of the reactors as well the product mixer. A perfect splitter is assumed in that all of the outlet streams have the same composition, temperature, and density as the feed stream.

Feed Splitter:

$$F^a_r = \sum_{k\in K}(F^{ab}_{r,k} + F^{ac}_{r,k}) + \sum_{l\in L}F^{ad}_{r,l} \quad \forall r \in R \tag{19}$$

CFR main outlet splitter:

$$F^e_k = \sum_{k'\in K}(F^{eb}_{k,k'} + F^{ec}_{k,k'}) + \sum_{l\in L}F^{ed}_{k,l} + \sum_{p\in P}F^{eh}_{k,p} \quad \forall k \in K \tag{20}$$

CFR side outlet splitter:

$$F^f_k = \sum_{k'\in K}(F^{fb}_{k,k'} + F^{fc}_{k,k'}) + \sum_{l\in L}F^{fd}_{k,l} + \sum_{p\in P}F^{fh}_{k,p} \quad \forall k \in K \tag{21}$$

CSTR outlet splitter:

$$F^g_l = \sum_{k\in K}(F^{gb}_{l,k} + F^{gc}_{l,k}) + \sum_{l'\in L}F^{gd}_{l,l'} + \sum_{p\in P}F^{gh}_{l,p} \quad \forall l \in L \tag{22}$$

2.2.4 Mixers

The mixers are used to combine all the material prior to the reactor units and to blend the product. Material and energy balances are required for each of the mixers.

Mixers prior to the CFR side feed:

$$c^b_{k,i}F^b_k = \sum_{r\in R} c^a_{r,i}F^{ab}_{r,k} + \sum_{k'\in K}(c^e_{k',i}F^{eb}_{k',k} + c^f_{k',i}F^{fb}_{k',k}) + \sum_{l\in L} c^g_{l,i}F^{gb}_{l,k} \quad \forall i\in I \quad \forall k\in K \tag{23}$$

$$H^b_k\rho^b_kF^b_k = \sum_{r\in R} H^a_r\rho^a_rF^{ab}_{r,k} + \sum_{k'\in K}(H^e_{k'}\rho^e_{k'}F^{eb}_{k',k} + H^f_{k'}\rho^f_{k'}F^{fb}_{k',k}) + \sum_{l\in L} H^g_l\rho^g_lF^{gb}_{l,k} \quad \forall k\in K \tag{24}$$

Mixers prior to the CFR main feed:

$$c^c_{k,i}F^c_k = \sum_{r\in R} c^a_{r,i}F^{ac}_{r,k} + \sum_{k'\in K}(c^e_{k',i}F^{ec}_{k',k} + c^f_{k',i}F^{fc}_{k',k}) + \sum_{l\in L} c^g_{l,i}F^{gc}_{l,k} \quad \forall i\in I \quad \forall k\in K \tag{25}$$

$$H^c_k\rho^c_kF^c_k = \sum_{r\in R} H^a_r\rho^a_rF^{ac}_{r,k} + \sum_{k'\in K}(H^e_{k'}\rho^e_{k'}F^{ec}_{k',k} + H^f_{k'}\rho^f_{k'}F^{fc}_{k',k}) + \sum_{l\in L} H^g_l\rho^g_lF^{gc}_{l,k} \quad \forall k\in K \tag{26}$$

Mixers prior to the CSTR feed:

$$c^d_{l,i}F^d_l = \sum_{r\in R} c^a_{r,i}F^{ad}_{r,l} + \sum_{k\in K}(c^e_{k,i}F^{ed}_{k,l} + c^f_{k,i}F^{fd}_{k,l}) + \sum_{l'\in L} c^g_{l',i}F^{gd}_{l',l} \quad \forall i\in I \quad \forall l\in L \tag{27}$$

$$H^d_l\rho^d_lF^d_l = \sum_{r\in R} H^a_r\rho^a_rF^{ad}_{r,l} + \sum_{k\in K}(H^e_k\rho^e_kF^{ed}_{k,l} + H^f_k\rho^f_kF^{fd}_{k,l}) + \sum_{l'\in L} H^g_{l'}\rho^g_{l'}F^{gd}_{l',l} \quad \forall l\in L \tag{28}$$

Product mixers:

$$c^h_{p,i}F^h_p = \sum_{k\in K}(c^e_{k,i}F^{eh}_{k,p} + c^f_{k,i}F^{fh}_{k,p}) + \sum_{l\in L} c^g_{l,i}F^{gh}_{l,p} \quad \forall i\in I \quad \forall p\in P \tag{29}$$

$$H^h_p\rho^h_pF^h_p = \sum_{k\in K}(H^e_k\rho^e_kF^{eh}_{k,p} + H^f_k\rho^f_kF^{fh}_{k,p}) + \sum_{l\in L} H^g_l\rho^g_lF^{gh}_{l,p} \quad \forall p\in P \tag{30}$$

2.2.5 Closure Relations

To fully specify the model, closure relationships that determine the density and enthalpy of the various streams are needed. These relationships are the equations of state for the density and enthalpy. They are generally functions of pressure P, temperature, T, and composition or mole fraction, x_i:

$$\rho = f^\rho(P, T, x_i) \tag{31}$$

$$H = f^h(P, T, x_i) \tag{32}$$

To determine the volumetric flowrates of the various streams and obtain total material balances, one additional expression is necessary. Provided that the density is in units of moles per volume, the sum of the concentrations is equal to the molar density:

$$\rho = \sum_{i \in I} c_i \tag{33}$$

Mole fractions are obtained from the concentrations using the expression

$$x_i = \frac{c_i}{\sum_{i'} c_{i'}} = \frac{c_i}{\rho} \tag{34}$$

A similar derivation is possible using the total molar flow and molar compositions instead of volumetric flow and concentrations. The primary difference would be that the concentrations would need to be determined from the molar composition and density.

2.2.6 Volume Scaling

The independent variables for the differential equations in the model are the reactor volumes, V. In general, these volumes will be different for each reactor and need to be optimized. Since the optimization of the independent variables in the differential system complicates the solution procedure, the reactor volumes are scaled and a different scaling factor is used for each reactor. The volume is scaled using the following expression:

$$V = V_k^t \bar{V} \quad \forall k \in K \tag{35}$$

where V_k^t is the scaling parameter and $\bar{V}$ is the scaled volume and the new independent variable. Thus, the differential is expressed as

$$dV = V_k^t d\bar{V} \tag{36}$$

By setting the bounds on the scaled volume to be 0 and 1, the scaling parameter V_k^t is also the volume of reactor k.

In Appendices A and B, the superstructure formulations based on the simplifying assumptions of constant density and ideal gas are presented respectively.

2.3 Optimal Control Formulation

The problem formulation consists of an objective function, dynamic constraints, time invariant constraints, initial conditions, and point constraints. This dynamic optimization problem is formulated as an optimal control problem by selecting appropriate control variables. The number of control variables that can be selected matches the degrees of freedom for the dynamic model. The dynamic equations, dynamic variables, and the sizes of each are listed in Table 3. There are $9K + 2I \times K + J \times K$ equations and $14K + 2I \times K + J \times K$ variables giving $5K$ degrees of freedom. Since each CFR in the model has an independent

Table 3: Number of dynamic equations and variables in the model.

Equations	Size	Variables	Size
CFR summation of concentrations	K	F_k^t	K
CFR material balance	$I \times K$	$c_{k,i}^t$	$I \times K$
CFR energy balance	K	H_k^t	K
CFR density equation of state	K	ρ_k^t	K
CFR enthalpy equation of state	K	T_k^t	K
		P_k^t	K
CFR feed sidestream material balance	K	F_k^s	K
CFR exit sidestream summation of concentrations	K	F_k^o	K
CFR exit sidestream material balance	$I \times K$	$c_{k,i}^o$	$I \times K$
CFR exit sidestream energy balance	K	H_k^o	K
CFR exit sidestream density equation of state	K	ρ_k^o	K
CFR exit sidestream enthalpy equation of state	K	T_k^o	K
		P_k^o	K
CFR reaction rates	$J \times K$	$r_{k,i}^t$	$J \times K$
		$\bar{F}_k^s$	K
		$\bar{F}_k^o$	K
		Q_k^t	K

set of equations, each with 5 degrees of freedom, 5 control variables must be selected for each CFR from the set of dynamic variables. The natural selection for the control variables are those which represent quantities that can be manipulated such as flow rates or temperatures. The pressure is often fixed thus eliminating two degrees of freedom. One possible set of control variables are the sidestream flowrates, F_k^s and F_k^o, and the CFR temperature T_k^t. There are other possible choices for the control variables. For example, the heat load, Q_k^t could be chosen instead of the temperature.

2.4 General Model Representation

For the purposes of the development of the solution algorithm, it is convenient to express the problem in the following general form:

$$\begin{array}{rrcl} \min & J(\dot{\boldsymbol{z}}(t_i), \boldsymbol{z}(t_i), \boldsymbol{u}(t_i), \boldsymbol{x}) & & \\ \text{s.t.} & \boldsymbol{f}(\dot{\boldsymbol{z}}(t), \boldsymbol{z}(t), \boldsymbol{u}(t), \boldsymbol{x}, t) & = & \mathbf{0} \\ & \boldsymbol{c}(\boldsymbol{z}(t_0), \boldsymbol{x}) & = & \mathbf{0} \\ & \boldsymbol{h}'(\dot{\boldsymbol{z}}(t_i), \boldsymbol{z}(t_i), \boldsymbol{u}(t_i), \boldsymbol{x}) & = & \mathbf{0} \\ & \boldsymbol{g}'(\dot{\boldsymbol{z}}(t_i), \boldsymbol{z}(t_i), \boldsymbol{u}(t_i), \boldsymbol{x}) & \leq & \mathbf{0} \\ & \boldsymbol{h}''(\boldsymbol{x}) & = & \mathbf{0} \\ & \boldsymbol{g}''(\boldsymbol{x}) & \leq & \mathbf{0} \\ & \boldsymbol{x} & \in & \mathcal{X} \subseteq \mathbb{R}^p \\ & t_i & \in & [t_0, t_N] \end{array} \tag{37}$$

where J is the objective function, $\boldsymbol{f}$ is the set of dynamic state equations, $\boldsymbol{c}$ are the initial conditions, $\boldsymbol{g}'$ and $\boldsymbol{h}'$ are the point constraints, and $\boldsymbol{g}''$ and $\boldsymbol{h}''$ are the general algebraic constraints. For the variables in the problem $\boldsymbol{x}$ is the vector of time invariant continuous variables, $\boldsymbol{z}$ is the vector of dynamic state variables, and $\boldsymbol{u}$ is the vector of control variables. The independent variable is t which corresponds to the scaled volumetric position along the reactor ($\bar{V}$).

3 Solution Methodology

The optimal control problem (37) is an optimization where the decisions are the control functions $\boldsymbol{u}(t)$ and the $\boldsymbol{x}$ variables. In finite dimensional nonlinear optimization, the decision space is equivalent to the number of decision variables. Since the time varying control functions require an infinite number of continuous decision variables for their representation, the optimal control problem is an infinite dimensional optimization. There are several ways to solve optimal control problems. These methods are (a) the solution of the necessary conditions, (b) dynamic programming, (c) complete discretization, and (d) control parameterization. The solution of the necessary conditions and the application of Pontryagin's maximum principle as described in Bryson and Ho[24] leads to the solution of two-point boundary value problems. Dynamic programming approaches employing grids for both the state and control variables have been proposed and applied to various systems[25;26;27;28]. Complete discretization methods discretize all the dynamic equations with respect to all dynamic variables. The DAEs are thus transformed into algebraic equations, and the problem can be solved using nonlinear programming techniques. Finite element collocation techniques were proposed by Cuthrell and Biegler[29] for the full discretization of DAE problems. The collocation methods were extended in Logsdon and Biegler[30] and Vasantharajan and Biegler [31] to include appropriate error constraints. The control parameterization techniques apply discretization only to the control variables. The problem is formulated as an NLP where the control parameters are determined through the optimization procedure and the DAE system is solved through an integration technique. This approach and its application to DAE problems has been studied by Vassiliadis et. al.[32;33].

The last two approaches, collocation and control parameterization, are widely used in the solution of optimization problems involving DAEs. The collocation methods have the advantage of optimizing the objective function and reducing the violation of the constraints simultaneously. This can reduce the overall computational cost of solving the problem. Another advantage is that the entire formulation is an independent NLP which facilitates the incorporation of general constraints. The disadvantage of the full discretization methods is that the number of variables in the NLP formulation becomes very large as the number of state variables in the problem increases. This method also requires a fixed number of discretization elements, and it leads to ill-conditioning of the NLP when stiff models are considered.

The control parameterization method is a sequential approach where the solution of the DAEs is decoupled from the NLP optimization. The DAEs are integrated along with the variational equations in order to obtain the required solution and gradient information. Although the solution of the DAEs can be computationally expensive, by decoupling them from

the optimization problem, the algorithm utilizes the features of the integration techniques. The state-of-the-art integrators can automatically adjust the number and size of the steps to handle the stiffness of the DAEs and well-suited for handling large, complex DAE models.

These two methods have their similarities as well. Whereas the state variables are explicitly discretized in the full collocation technique, the control parameterization method uses integration to solve the DAEs which essentially also discretizes the state variables. This similarity is enhanced by the fact that the full collocation can be shown to be equivalent to a Runge-Kutta scheme. The Backwards Difference Formula (BDF) methods for integration tend to be more robust and efficient than Runge-Kutta methods. Using the control parameterization method with the integration ensures that the correct number of steps are taken and that the error criteria are satisfied.

Due to the advantages of the control parameterization approach, it is applied to solve the optimal control problem in this work. The application of control parameterization techniques for process synthesis is described by Schweiger and Floudas[34] where the focus is on the interaction of design and control and the resulting problem is a mixed-integer optimal control problem. A similar methodology is used in this work for the solution of the reactor network synthesis problem.

3.1 Parameterization of the Optimal Control Problem

Applying control parameterization reduces the infinite dimensional optimal control problem to a finite dimensional problem. The basic idea behind the control parameterization is the express the control variables $\boldsymbol{u}(t)$ as functions of time invariant parameters. This parameterization can be done in terms of the independent variable t which is described by an appropriate open loop control law:

$$\boldsymbol{u}(t) = \boldsymbol{\phi}(\boldsymbol{w}, t) \tag{38}$$

A convenient choice for the control parameterization function $\boldsymbol{\phi}(\boldsymbol{w}, t)$ is the Lagrange polynomial. These are interpolating functions where the parameters are node values that determine the shape of the function and are used as optimization variables. The time horizon is divided into intervals with the controls defined as polynomials over each interval. The Lagrange polynomial expression of order M in interval i has the form

$$\begin{aligned} \boldsymbol{\phi}_i(\boldsymbol{w}, t) &= \sum_{j=1}^{n} \boldsymbol{w}_{ij} && \text{for} \quad M = 1 \\ \boldsymbol{\phi}_i(\boldsymbol{w}, t) &= \sum_{j=1}^{n} \boldsymbol{w}_{ik} \prod_{k=1, k\neq j}^{M} \frac{\bar{t}-\bar{t}_k}{\bar{t}_j-\bar{t}_k} && \text{for} \quad M \geq 2 \end{aligned} \tag{39}$$

where $\bar{t}$ is the normalized time over the interval i

$$\bar{t} = \frac{t - t_{i-1}}{t_i - t_{i-1}} \tag{40}$$

This parameterization allows for polynomial expressions of various order to be used. For example, a piecewise linear expression with continuity between the intervals is expressed as

$$\boldsymbol{\phi}_i = \boldsymbol{w}_i \frac{\bar{t} - \bar{t}_{i+1}}{\bar{t}_i - \bar{t}_{i+1}} + \boldsymbol{w}_{i+1} \frac{\bar{t} - \bar{t}_i}{\bar{t}_{i+1} - \bar{t}_i} \tag{41}$$

Since the control parameters change from one interval to the next, discontinuities arise in the DAE system.

In the reactor network synthesis problem the reactor volume needs to be optimized. This volume is determined by the limits on the integration which are fixed in the control parameterization approach. To allow the volume to vary, the independent variable is scaled and the integration is performed over this scaled variable. The scaling factor becomes a variable which can be optimized. For example, consider the differential equation

$$\frac{dz}{dt} = f(z, x)$$

The variable t can be scaled using the relation

$$t = \tau \bar{t}$$

where $\bar{t}$ is the scaled time and τ is the scaling factor. Substituting this into the differential equation results in

$$\frac{dz}{d\bar{t}} = \tau f(z, x)$$

where τ is now a variable for the optimization. By choosing the limits of the scaled time in an interval to be 0 and 1, the scaling parameter becomes the true size of the integration horizon, which is the volume of the CFR. Scaling factors, τ_i are introduced to allow the size of the each interval to vary. If the scaled size of each interval is one, then the true total size is the sum of the scale factors for each interval. Note that this scaling affects the dynamic equations which explicitly depend on time. The real time must be determined from the sizes of the intervals and the scaling factors for each interval.

The set of time invariant parameters $\boldsymbol{x}$ is now expanded to include the control parameters:

$$\boldsymbol{x} = \{\boldsymbol{x}, \boldsymbol{w}\} \tag{42}$$

The set of DAEs ($\boldsymbol{f}$) is expanded to include parameterization functions

$$\boldsymbol{f}(\cdot) = \{\boldsymbol{f}(\cdot), \boldsymbol{\phi}(\cdot)\} \tag{43}$$

and the control variables are converted to dynamic state variables:

$$\boldsymbol{z} = \{\boldsymbol{z}, \boldsymbol{u}\} \tag{44}$$

Through the application of the control parameterization, the control variables are effectively removed from the problem and the following NLP/DAE results:

$$\begin{array}{rrcl} \min & J(\dot{\boldsymbol{z}}(t_i), \boldsymbol{z}(t_i), \boldsymbol{x}) & & \\ \text{s.t.} & \boldsymbol{f}(\dot{\boldsymbol{z}}(t), \boldsymbol{z}(t), \boldsymbol{x}, t) & = & \boldsymbol{0} \\ & \boldsymbol{c}(\boldsymbol{z}(t_0), \boldsymbol{x}) & = & \boldsymbol{0} \\ & \boldsymbol{h}'(\dot{\boldsymbol{z}}(t_i), \boldsymbol{z}(t_i), \boldsymbol{x}) & = & \boldsymbol{0} \\ & \boldsymbol{g}'(\dot{\boldsymbol{z}}(t_i), \boldsymbol{z}(t_i), \boldsymbol{x}) & \leq & \boldsymbol{0} \\ & \boldsymbol{h}''(\boldsymbol{x}) & = & \boldsymbol{0} \\ & \boldsymbol{g}''(\boldsymbol{x}) & \leq & \boldsymbol{0} \\ & \boldsymbol{x} & \in & \mathcal{X} \subseteq \mathbb{R}^p \\ & t_i & \in & [t_0, t_N] \end{array} \tag{45}$$

This problem is an optimization in the space of the $\boldsymbol{x}$ variables where J, $\boldsymbol{g}'$, and $\boldsymbol{h}'$, are implicit functions of $\boldsymbol{x}$ variables through the solution of the DAE system.

3.2 Solution of NLP/DAE

Standard gradient based methods for solving NLPs such as reduced gradient methods, conjugate gradient methods, sequential quadratic programming methods, require function evaluations along with the gradient evaluations. For this problem, the function evaluations and gradients with respect to $\boldsymbol{x}$ are required for J, $\boldsymbol{h}'$, $\boldsymbol{g}'$, $\boldsymbol{h}''$, and $\boldsymbol{g}''$. For $\boldsymbol{h}''$, and $\boldsymbol{g}''$, analytical expressions can be obtained. However, for J, $\boldsymbol{h}'$, $\boldsymbol{g}'$ the function evaluations and gradients are determined as implicit functions of $\boldsymbol{x}$ through the solution of the DAE system. Integrating the DAE system along with the variational equations provides the values of the state variables at the time instances, $\boldsymbol{z}(t_i)$, as well as the gradients $\frac{d\boldsymbol{z}}{d\boldsymbol{x}}$. With this information known, the functions J, $\boldsymbol{g}'$, and $\boldsymbol{h}'$ are evaluated directly, and the gradients are determined by applying the chain rule:

$$\begin{aligned}
\frac{dJ}{d\boldsymbol{x}} &= \left(\frac{\partial J}{\partial \boldsymbol{z}}\right)\left(\frac{\partial \boldsymbol{z}}{\partial \boldsymbol{x}}\right) + \left(\frac{\partial J}{\partial \boldsymbol{x}}\right) \\
\frac{d\boldsymbol{h}'}{d\boldsymbol{x}} &= \left(\frac{\partial \boldsymbol{h}'}{\partial \boldsymbol{z}}\right)\left(\frac{\partial \boldsymbol{z}}{\partial \boldsymbol{x}}\right) + \left(\frac{\partial \boldsymbol{h}'}{\partial \boldsymbol{x}}\right) \\
\frac{d\boldsymbol{g}'}{d\boldsymbol{x}} &= \left(\frac{\partial \boldsymbol{g}'}{\partial \boldsymbol{z}}\right)\left(\frac{\partial \boldsymbol{z}}{\partial \boldsymbol{x}}\right) + \left(\frac{\partial \boldsymbol{g}'}{\partial \boldsymbol{x}}\right)
\end{aligned} \tag{46}$$

With all of the function evaluations and gradients known, the problem can be solved using existing local NLP optimization codes.

4 Algorithmic Framework

The proposed algorithm for the solution of the general optimal control formulation has been implemented in the software package MINOPT[35;36]. MINOPT is a general purpose optimization package capable of addressing a wide variety of problem types described by the types of variables and constraints used in the problem. MINOPT handles the following types of variables:

- Continuous time invariant variables
- Continuous dynamic variables
- Control variables
- Integer variables

and the following types of constraints:

- Linear
- Nonlinear

- Dynamic
- Dynamic Piecewise Continuous
- Dynamic Point
- Dynamic Path

MINOPT can address the following classes of problems:

- Linear Programs (LP)
- Mixed Integer Linear Programs (MILP)
- NonLinear Programs (NLP)
- Mixed Integer NonLinear Programs (MINLP)
- Dynamic Simulations
- Optimal Control Problems (OCP)
- Mixed Integer Optimal Control Problems (MIOCP)

The class of problems which are of importance for the purposes of this work are the optimal control problem. Note that MINOPT is also capable of handling optimal control problems involving discrete decisions (MIOCPs).

MINOPT has two phases: first, the problem information is read and stored, and second, the problem is solved. The first phase features a parser which reads all of the problem information from an input file. The input file is written in a specific modeling language which has a clear syntax and allows the user to enter the problem in a concise format. The input file includes information such as variable names, variable partitioning, parameter definitions, option specifications, and constraint definitions. The parser features index notation for compact constraint notation, the ability to recognize and handle the various constraint types, and the capability of determining the analytical Jacobian information by employing automatic differentiation.

After the problem information has been determined, MINOPT employs the appropriate algorithm to solve the problem. For the solution of the various problems and subproblems, MINOPT interfaces with existing software. The types of problems and the solvers implemented in MINOPT are shown in Table 4. The flow of the program is shown in Figure 5.

Many complex reaction mechanisms have numerous reactions and species. Keeping track of the many different parameters associated with the problem can be difficult. The Chemkin package[37] has been developed to help simplify the task of formulating and solving problems involving gas-phase chemical kinetics. MINOPT has a connection to Chemkin through which it can obtain all of the details of the reaction mechanism and use them in the model formulation.

MINOPT is available through Princeton University and information regarding the software can be obtained at http://titan.princeton.edu/MINOPT.

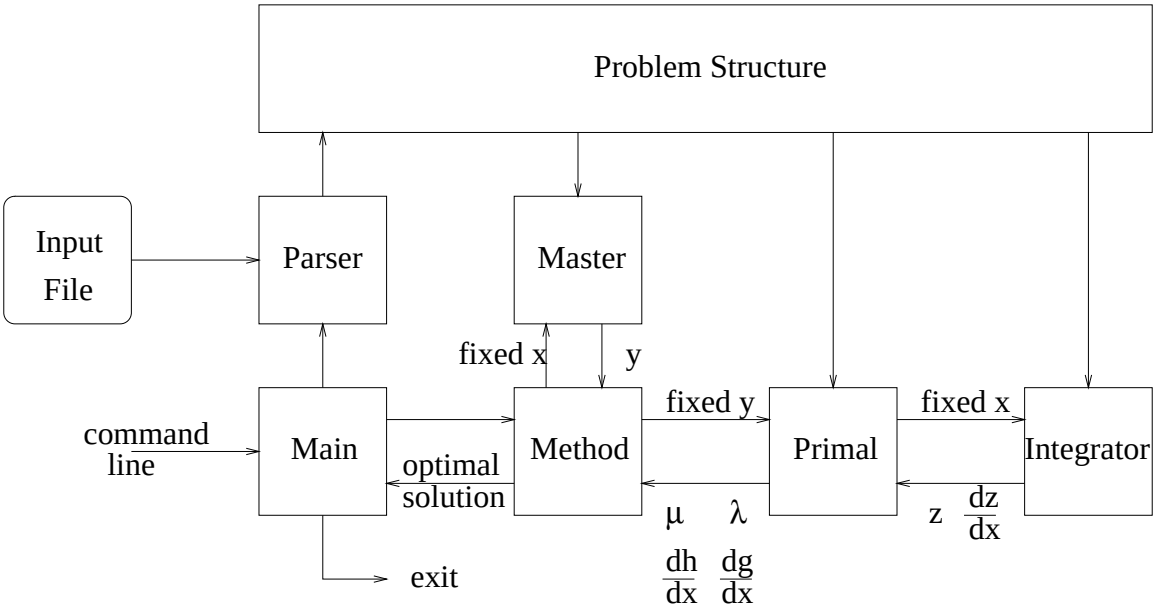

Figure 5: Program flow for MINOPT.

Table 4: Solvers implemented in MINOPT.

Problem Type	Algorithm	Solver
LP	Simplex method	CPLEX[38]
		MINOS[39]
		LSSOL[40]
MILP	Branch and Bound	CPLEX[38]
NLP	Augmented Lagrangian/Reduced Gradient	MINOS[39]
	Sequential Quadratic Programming	NPSOL[41]
	Sequential Quadratic Programming	SNOPT[42]
Dynamic	Integration (Backward Difference Formula)	DASOLV[43]
	Integration (Backward Difference Formula)	DASSL[44]
MINLP	Generalized Benders Decomposition	MINOPT
	Outer Approximation/Equality Relaxation	MINOPT
	Outer Approximation/Augmented Penalty	MINOPT

5 Computational Studies

The proposed approach has been applied to numerous examples ranging from the simpler constant density isothermal and nonisothermal mechanisms involving three reactions to complex nonisothermal mechanisms involving many species and reactions where the kinetic and thermodynamic data are obtained through Chemkin.

The superstructure used for the examples consists of a CFR and CSTR as shown in Figure 3. The control variables selected for the CFRs are the sidestream flowrates and the temperature in the reactor. For the control parameterization, piecewise linear functions are used for the sidestream flowrates and piecewise quadratic functions with continuous first derivatives are used for the temperature profiles. The time horizon is divided into ten intervals for the control parameterization.

Both the relative and absolute NLP optimization tolerances were set to 1×10^{-6} and the integration tolerance was set to 1×10^{-8}. All problems were solved on an HP C-160.

5.1 Isothermal Examples

The first set of examples are isothermal problems. The temperature dependence is removed from modeling equations and the energy balances are not included. All of the isothermal examples are also constant density. For each problem, the reaction mechanism, the stoichiometric coefficient matrix, reaction types, kinetic parameters, and feed conditions are given.

5.1.1 Example 1—Isothermal Van de Vusse Reaction

The Van de Vusse reaction mechanism has four species and three reactions:

$$\mathbf{A} \xrightarrow{\mathbf{k_1}} \mathbf{B} \xrightarrow{\mathbf{k_2}} \mathbf{C}$$
$$\mathbf{2A} \xrightarrow{\mathbf{k_3}} \mathbf{D}$$

where the rate expressions are

$$\begin{aligned} f_1^r &= k_1 c_A \\ f_2^r &= k_2 c_B \\ f_3^r &= k_3 c_A^2 \end{aligned}$$

and the stoichiometric matrix for this mechanism is

$$\nu = \begin{bmatrix} -1 & 0 & -2 \\ 1 & -1 & 0 \\ 0 & 1 & 0 \\ 0 & 0 & 1 \end{bmatrix}$$

The feed is pure **A**, the desired product is the intermediate **B**, and the objective is to maximize the yield of **B**. The problem has 93 variables (16 dynamic) and 79 constraints. Four different cases are studied where each involves a different set of parameters as shown in Table 5.

Table 5: Parameters for isothermal Van de Vusse reaction.

Parameter	Case 1	Case 2	Case 3	Case 4
k_1 [s^{-1}] (first order)	10	10	10	1
k_2 [s^{-1}] (first order)	1	1	1	2
k_3 [L/(mol s)] (second order)	0.5	0.25	0.5	10
Feed flowrate [L/s] (pure **A**)	100	100	100	100
Feed concentration [mol **A**/L]	0.58	0.58	5.8	1.0

For Cases 1 and 2, the solution is found to be a single PFR whereas for Cases 3 and 4, the optimal reactor network is found to be a CSTR in series with a PFR. The reactor network solutions for Cases 3 and 4 are shown in Figures 6 and 7. The results for all of the cases using the proposed approach and the results of previous work are shown in Table 6. In all of the cases, an improved solution has been found in comparison to previous work. This is attributed to the fact that no approximation is made in the modeling of the PFR.

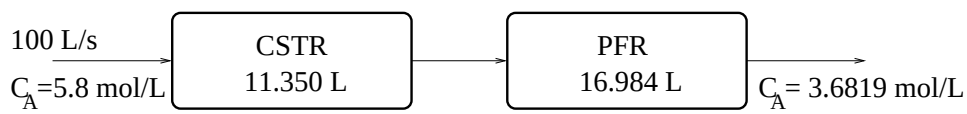

Figure 6: Reactor network solution for the isothermal Van de Vusse reaction—Case 3.

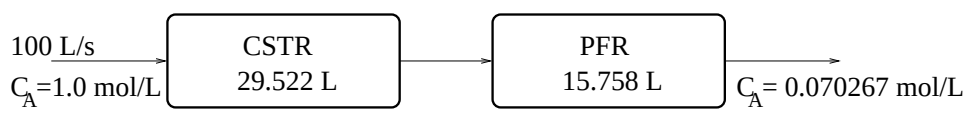

Figure 7: Reactor network solution for isothermal Van de Vusse reaction—Case 4.

5.1.2 Example 2—Isothermal Trambouze Reaction

The Trambouze reaction involves a zero order, a first order, and a second order reaction all in parallel:

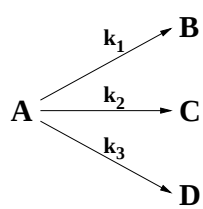

The rate expressions are

$$
\begin{aligned}
f_1^r &= k_1 c_A \\
f_2^r &= k_2 c_B \\
f_3^r &= k_3 c_A^2
\end{aligned}
$$

Table 6: Summary of results for the isothermal Van de Vusse reaction.

Reference	Objective	Solution[1]
	Case 1	
Chitra and Govind[45]	0.4362 mol/L	PFR
Achenie and Biegler[8]	0.4368 mol/L	PFR (29.65 L)
Kokossis and Floudas[10]	0.4364 mol/L	PFR (25.396 L)
Proposed Approach	0.43708 mol/L	PFR (25.335 L)
	Case 2	
Achenie and Biegler[18]	0.4391 mol/L	(0.2370 s)
Balakrishna and Biegler[19]	0.4429 mol/L	(0.288 s)
Lakshmanan and Biegler[22]	0.4269 mol/L	PFR (0.262 s)
Proposed Approach	0.44297 mol/L	PFR (25.458 L)
	Case 3	
Chitra and Govind[45]	3.6772 mol/L	PFR
Kokossis and Floudas[10]	3.6796 mol/L	CSTR (11.382 L) + PFR (16.989 L)
Proposed Approach	3.6819 mol/L	CSTR (11.350 L) + PFR (16.984 L)
	Case 4	
Balakrishna and Biegler[19]	0.069 mol/L	RR (0.1005 s) + PFR (0.09 s)
Lakshmanan and Biegler[22]	0.0703 mol/L	CSTR (0.302 s) + PFR (0.161s)
Proposed Approach	0.070267 mol/L	CSTR (29.522 L) + PFR (15.758 L)

[1]Solutions are reported in terms of the reactors in the flowsheet along with their volume (L) or space time (s).

The stoichiometric matrix is

$$\nu = \begin{bmatrix} -1 & -1 & -1 \\ 1 & 0 & 0 \\ 0 & 1 & 0 \\ 0 & 0 & 1 \end{bmatrix}$$

The parameters for this example are given in Table 7. The objective is to maximize the selectivity of **C** to **A** which is defined as $C_C/(1 - C_A)$.

Table 7: Parameters for the Trambouze reaction.

Parameter	Value
k_1	0.025 mol/(L min) (zero order)
k_2	0.2 min^{-1} (first order)
k_3	0.4 L/(mol min) (second order)
Feed flowrate	100 L/min pure **A**
Feed concentration	1.0 mol/L

This problem is noted for having multiple solutions. In Kokossis and Floudas[10] three different structures were found each with the same selectivity of 0.500 and the authors indicated that there are infinitely many solutions. In this work, numerous solutions have been obtained. One extreme solution is a single 750 L CSTR where the product concentrations for C_C and C_A are 0.375 mol/L and 0.25 mol/L respectively. Another extreme solution is a single differential sidestream reactor with a linear feed profile along the reactor. All of the feed is fed to the side feed for the CFR and fed linearly with respect to the position along the reactor. Other solutions involving both types of reactors, recycles, and bypasses have also been obtained.

5.1.3 Example 3—Isothermal α-Pinene Reaction

The reaction mechanism for the conversion of α-pinene to several products takes place through the following scheme:

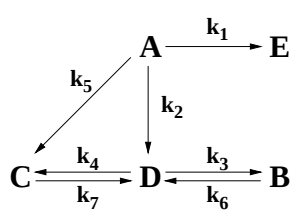

The rate expressions are

$$
\begin{aligned}
f_1^r &= k_1 c_A \\
f_2^r &= k_2 c_A \\
f_3^r &= k_3 c_D \\
f_4^r &= k_4 c_D^2 \\
f_5^r &= k_5 c_A^2 \\
f_6^r &= k_6 c_B \\
f_7^r &= k_7 c_C
\end{aligned}
$$

The stoichiometric matrix for this mechanism is

$$
\nu_{i,j} = \begin{bmatrix}
-1 & -1 & 0 & 0 & -2 & 0 & 0 \\
0 & 0 & 1 & 0 & 0 & -1 & 0 \\
0 & 0 & 0 & 1 & 1 & 0 & -1 \\
0 & 1 & -1 & -2 & 0 & 1 & 2 \\
1 & 0 & 0 & 0 & 0 & 0 & 0
\end{bmatrix}
$$

and the parameters are given in Table 8. The objective is to maximize the selectivity of **C** to **D** which is defined as C_C/C_D. The volume of the reaction for this example is constrained to 6000 L and the minimum concentration of **D** in the product is 0.01 mol/L. The problem has 110 variables (22 dynamic) and 97 constraints.

Table 8: Parameters for isothermal α-pinene reaction.

Parameter	Value
k_1	0.33384 s^{-1} (first order)
k_2	0.26687 s^{-1} (first order)
k_3	0.14940 s^{-1} (first order)
k_4	0.18957 L/(mol s) (second order)
k_5	0.009598 L/(mol s) (second order)
k_6	0.29425 s^{-1} (first order)
k_7	0.011932 s^{-1} (first order)
Feed Flowrate	100 L/s (pure **A**)
Feed Concentration	1.0 mol/L **A**

The solution found as shown in Figure 8, consists of a single PFR with its volume at the upper limit of 6000 L and a bypass stream. The maximum selectivity is found to be 1.5570 and the CPU time required is 39.4s (HP C-160). These results are compared to those of previous work in Table 9.

Most of the previous approaches failed to identify the bypass stream in the solution. If no limit is placed on the size of the PFR, the value of the objective at equilibrium is 1.5570. If the volume of the reactor is constrained to 6000 L, the maximum value of the objective that can be achieved is 1.48 as equilibrium can not be obtained. The value of 1.5570 can be achieved by using a bypass stream. Because the objective is the ratio C_C/C_D, the overall

amount of conversion does not matter. By sending only a fraction of the feed to the PFR and allowing the reaction to reach equilibrium, the value of 1.5570 can be achieved for the PFR. When the exit stream from the PFR is mixed with the bypass stream, the ratio C_C/C_D does not change. Thus, the objective value of 1.5570 can be achieved for even smaller sizes of the PFR. As the reactor gets smaller, less of the feed is sent to the reactor so that equilibrium can be achieved and the objective value of 1.5570 can be maintained.

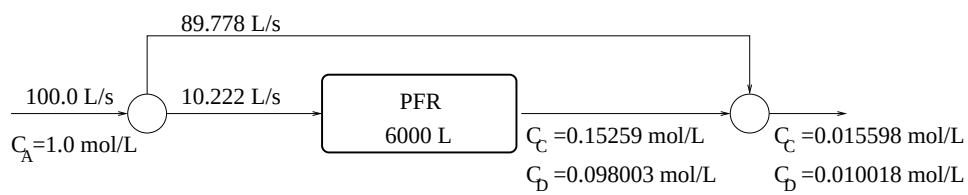

Figure 8: Reactor network solution for the α-pinene reaction.

Table 9: Summary of results for the Isothermal α-pinene reaction.

Reference	Maximum selectivity	solution
Kokossis and Floudas[10]	1.402	
Balakrishna and Biegler[19]	1.48	PFR (60 s)
Lakshmanan and Biegler[22]	1.48	PFR (60 s)
Proposed Approach	1.5570	PFR (6000 L) + bypass

5.1.4 Example 4—Isothermal Denbigh Reaction

The Denbigh reaction mechanism is

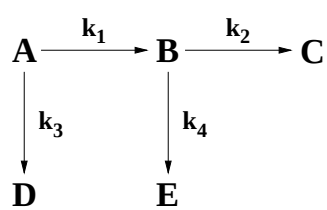

The rate expressions are

$$
\begin{aligned}
f_1^r &= k_1 c_A^2 \\
f_2^r &= k_2 c_B \\
f_3^r &= k_3 c_A \\
f_4^r &= k_4 c_B^2
\end{aligned}
$$

Two distinct cases are examined for this problem.

In the first case, the objective is to maximize the selectivity of **B** to **D** (C_B/C_D). The stoichiometric coefficient matrix is

$$\nu = \begin{bmatrix} -1 & 0 & -1 & 0 \\ 0.5 & -1 & 0 & -1 \\ 0 & 1 & 0 & 0 \\ 0 & 0 & 1 & 0 \\ 0 & 0 & 0 & 1 \end{bmatrix}$$

and the parameters are given in Table 10. This problem has 114 variables (19 dynamic) and 90 constraints. The optimal reactor network shown in Figure 9 is found to be a single PFR with a volume of 20.750 L. The objective value is 1.3218 and the solution is obtained in 113.33s of CPU time on an HP C-160.

Table 10: Parameters for isothermal Denbigh reaction.

Parameter	Value
k_1	1.0 L/(mol s) (second order)
k_2	0.6 s^{-1} (first order)
k_3	0.6 s^{-1} (first order)
k_4	0.1 L/(mol s) (second order)
Feed flowrate	100 L/s
Feed concentration	6.0 mol/L **A**, 0.6 mol/L **D**

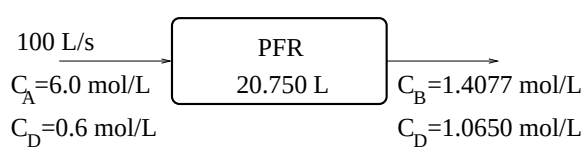

Figure 9: Reactor network solution to the Denbigh reaction—Case 1.

In the second case, The objective is to maximize the production of **C** subject to 95% conversion of **A**. A slightly different stoichiometric matrix is considered:

$$\nu = \begin{bmatrix} -1 & 0 & -1 & 0 \\ 1 & -1 & 0 & -1 \\ 0 & 1 & 0 & 0 \\ 0 & 0 & 1 & 0 \\ 0 & 0 & 0 & 1 \end{bmatrix}$$

The same rate constants are used as in Case 1, but the feed consists only of pure **A** with a concentration of 6.0 mol/L. Two CSTRs and one CFR are considered in the superstructure and the problem has 130 variables (19 dynamic) and 107 constraints.

The solution as shown in Figure 10 consists of a PFR with a volume of 73.563 L followed by a CSTR with a volume of 470140 L. The network involve a bypass stream and gives product concentrations of 0.300 mol/L **A**, 0.000808 mol/L **B**, 3.5399 mol/L of **C**, 1.6430 mol/L of **D**, and 0.51627 mol/L of **E**.

The results of the isothermal Denbigh reaction are summarized with those of previous work in Table 11.

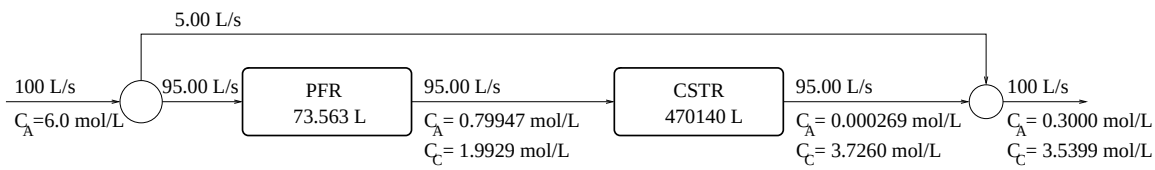

Figure 10: Reactor network solution to the Denbigh reaction—Case 2.

Table 11: Summary of results for the isothermal Denbigh reaction.

Reference	Objective	Solution
	Case 1	
Achenie and Biegler[18]	1.322	2 PFRs in series
Kokossis and Floudas[10]	1.319	PFR (20.7062 L)
Balakrishna and Biegler[19]	1.322	PFR (20.9 L)
Lakshmanan and Biegler[22]	1.322	PFR (20.9 L)
Proposed Approach	1.3218	PFR (20.750 L)
	Case 2	
Balakrishna and Biegler[19]	3.54 mol/L	PFR (0.766 s) + CSTR (3505 s)
Lakshmanan and Biegler[22]	3.54 mol/L	PFR (0.766 s) + CSTR (3505 s)
Proposed Approach	3.5399 mol/L	PFR (0.77435 s) + CSTR (4948.8 s)

5.2 Nonisothermal Examples

The next set of examples involves nonisothermal reaction kinetics. The ability to manipulate the temperature allows for control of the reaction rate and better control of the reactor concentrations. For most of these examples, the Arrhenius law is used to describe the temperature dependence:

$$k(T) = \hat{k}e^{\frac{E}{RT}}$$

5.2.1 Example 5—Nonisothermal Van de Vusse Reaction

In this example the same reaction scheme as in Example 1 is used, but the rate constants now depend on the temperature as defined by the Arrhenius law. Two cases are considered:

an exothermic reaction and an endothermic reaction. The objective for both cases is to maximize the yield of **B**. In both cases, the feed flowrate is 100 L/h of pure **A** with a concentration of 1 mol/L. For Case 1, the bounds on the temperature are 300° K and 810° K, and for Case 2 they are 450° K and 810° K. The parameters for both cases are given in Table 12.

Both cases are first solved using ten intervals of equal size for the control parameterization. The formulation has 118 variables (18 dynamic) and 90 constraints. Both cases are again solved using 10 individually scaled intervals which has 128 variables (18 dynamic) and 91 constraints.

Table 12: Parameters for the nonisothermal Van de Vusse reaction.

		$\hat{k}$	E	$\frac{\Delta H}{\rho C_p}$
Case 1:	1	5.4e9 h^{-1}	15.84 kcal/mol	-84 K L/mol
	2	1.6e12 h^{-1}	23.76 kcal/mol	-108 K L/mol
	3	3.6e5 L/(mol h)	7.92 kcal/mol	-60 K L/mol
Case 2:	1	5.4e9 h^{-1}	15.84 kcal/mol	84 K L/mol
	2	3.6e5 h^{-1}	7.92 kcal/mol	108 K L/mol
	3	1.6e12 L/(mol h)	23.76 kcal/mol	60 K L/mol

Nonisothermal Van de Vusse—Case 1: Exothermic reaction

Using the equally spaced intervals, the optimal network as shown in Figure 11 consists of a PFR with a volume of 2.4504 L followed by a CSTR with a volume at its upper bound of 10000 L. The maximum yield of **B** obtained is 0.82673 mol/L **B**. The temperature profile in the PFR as shown in Figure 12 initially falls sharply then rises and levels off. The concentration profiles are shown in Figure 13.

When the control intervals are individually scaled, the maximum yield of **B** obtained is 0.83913 mol/L. The solution as shown in Figure 14 is a single PFR with a sharply falling temperature profile followed by a CSTR. The PFR temperature profile is shown in Figure 15 and the concentration profile is shown in Figure 16. By allowing the size of each control interval to vary, the temperature is permitted to fall more sharply than in the case where the lengths are equal. Note that both constraints on the reactor volumes are active.

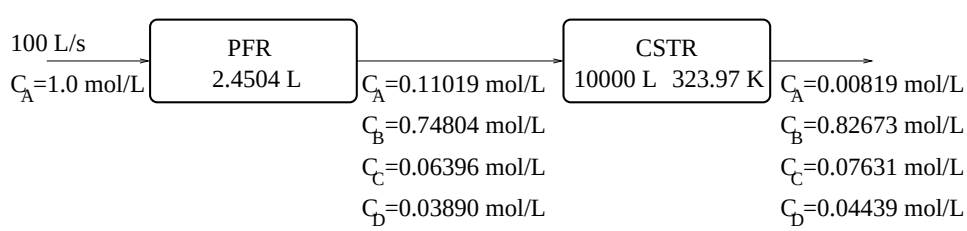

Figure 11: Reactor network solution for the nonisothermal Van de Vusse reaction—Case 1 (equally sized intervals).

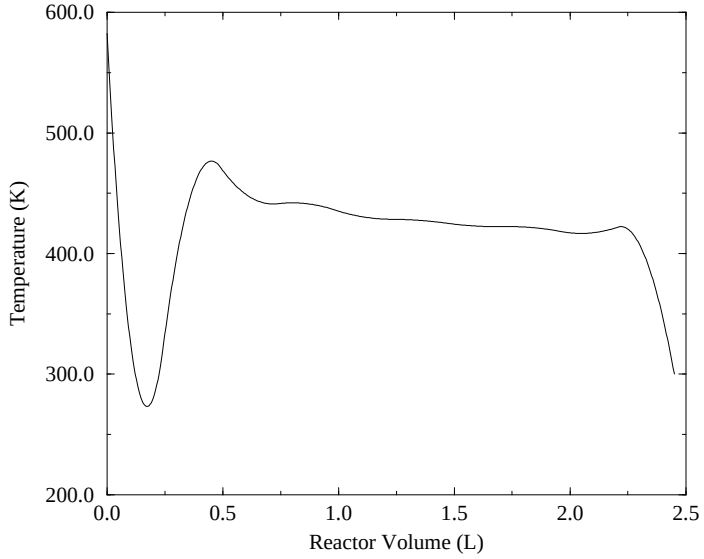

Figure 12: Temperature profile for the PFR in the nonisothermal Van de Vusse solution—Case 1 (equally sized intervals).

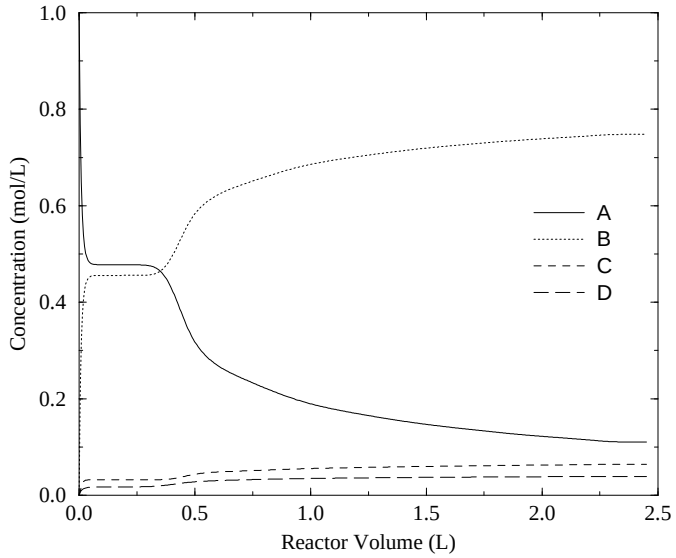

Figure 13: Concentration profile for the PFR in the nonisothermal Van de Vusse solution—Case 1 (equally sized intervals).

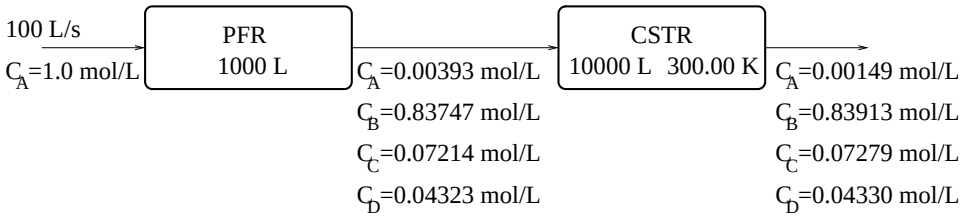

Figure 14: Reactor network solution for the nonisothermal Van de Vusse reaction—Case 1 (individually scaled intervals).

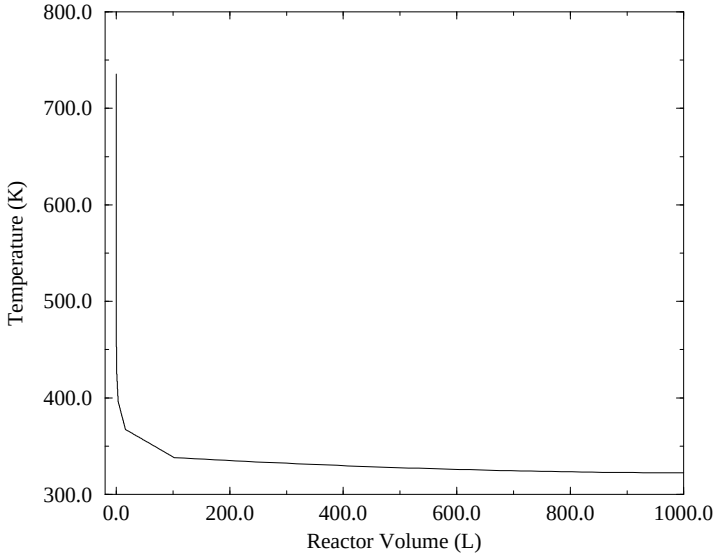

Figure 15: Temperature profile for the PFR in the nonisothermal Van de Vusse solution—Case 1 (individually scaled intervals).

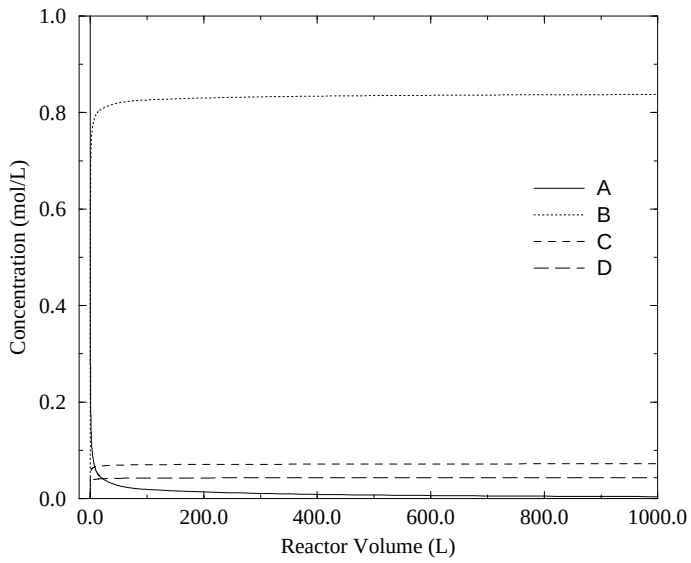

Figure 16: Concentration profile for the PFR in the nonisothermal Van de Vusse solution—Case 1 (individually scaled intervals).

Nonisothermal Van de Vusse—Case 2: Endothermic reaction

Using the equally sized intervals, the optimal network as shown in Figure 17 consists of a CSTR of volume 0.06756 L followed by a PFR with a volume of 0.08030 L. The temperature profile as shown in Figure 18 appears to rise in an exponential fashion. The concentration profiles are shown in Figure 19.

When the control intervals are individually scaled, the optimal network shown in Figure 20 consists of a single PFR with a sharply rising temperature profile. The temperature profile which is shown in Figure 21 starts at the lower bound of 450° K and stays there for approximately one third of the length of the reactor. At this point the temperature rises in a seemingly exponential fashion. The spike in the temperature profile corresponds to an control interval with a size of zero and has no effect on the concentration profiles which are shown in Figure 22.

The results for the nonisothermal Van de Vusse along with those of previous work are summarized in Table 13. Note that for Case 2, the results obtained by Chitra and Govind [46] were obtained by allowing the temperature to rise to 1265° K. If the upper bound on the temperature is increased to 1265° K, the optimal solution is a PFR with the temperature rising to its upper bound, and the maximum yield obtained improves to 0.8383 mol/L.

5.2.2 Example 6—Nonisothermal Parallel Reactions

This example is taken from Levenspiel[47] and involves two parallel reactions:

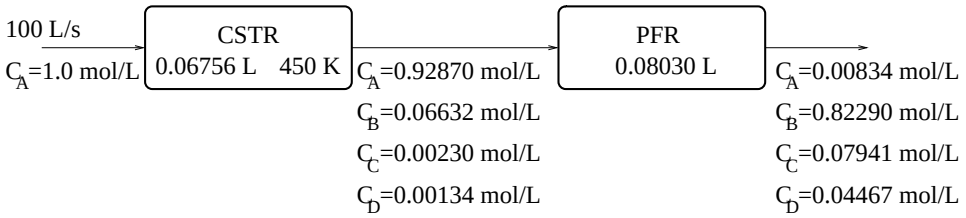

Figure 17: Reactor network solution for the nonisothermal Van de Vusse reaction—Case 2 (equally sized intervals).

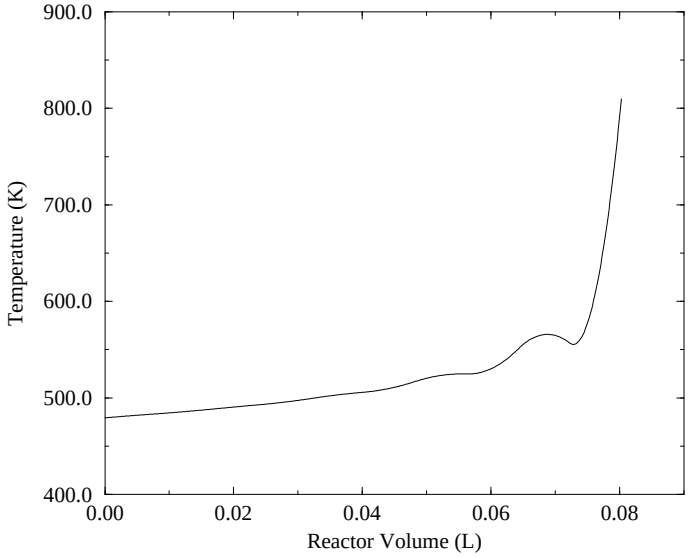

Figure 18: Temperature Profile for the PFR in the nonisothermal Van de Vusse solution—Case 2 (equally sized intervals).

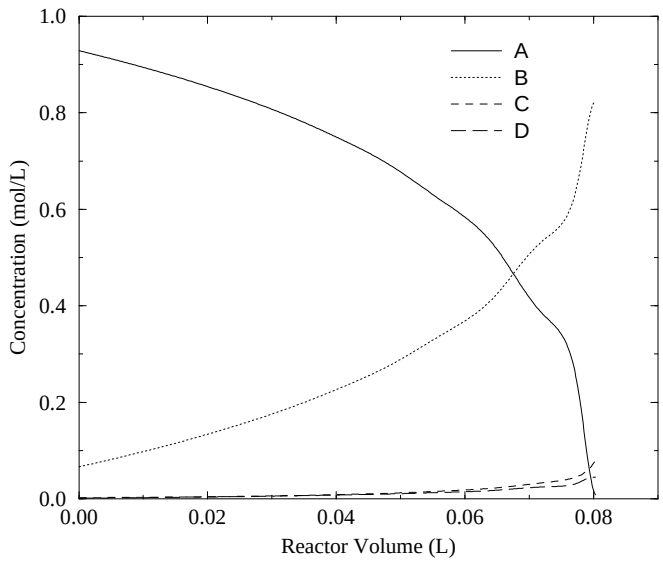

Figure 19: Concentration profiles for the PFR in the nonisothermal Van de Vusse solution—Case 2 (equally sized intervals).

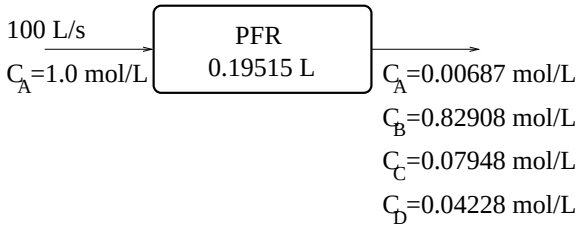

Figure 20: Reactor network solution for the nonisothermal Van de Vusse reaction—Case 2 (individually scaled intervals).

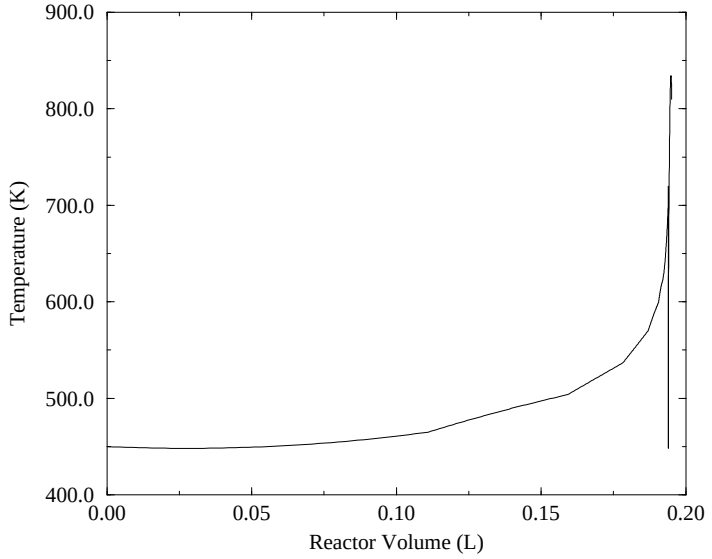

Figure 21: Temperature profile for the PFR in the nonisothermal Van de Vusse solution—Case 2 (individually scaled intervals).

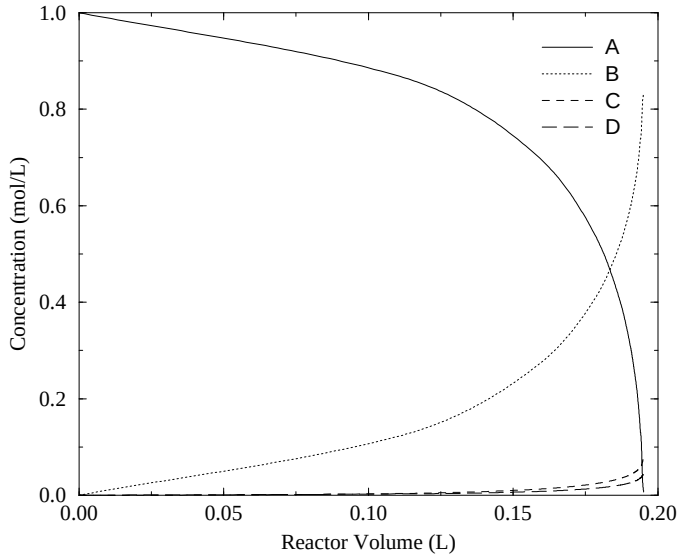

Figure 22: Concentration profiles for the PFR in the nonisothermal Van de Vusse solution—Case 2 (individually scaled intervals).

Table 13: Summary of results for the nonisothermal Van de Vusse reaction.

Reference	Objective	Solution
	Case 1	
Chitra and Govind[46]	0.822 mol/L	5 PFRs
Achenie and Biegler[9]	0.815 mol/L	5 PFRs (0.222s)
Balakrishna and Biegler[20]	0.786 mol/L	0.22 s
Kokossis and Floudas[12]	0.8414 mol/L	PFR
Proposed Approach (equally sized intervals)	0.82673 mol/L	PFR (2.4504 L) + CSTR (10000L)
Proposed Approach (individually scaled intervals)	0.83913 mol/L	PFR (1000 L) + CSTR (10000 L)
	Case 2	
Chitra and Govind[46]	0.834 mol/L	2 PFRs + 2 RRs + CSTR
Achenie and Biegler[9]	0.183 mol/L	2 PFRs (0.515 s)
Kokossis and Floudas[12]	0.764 mol/L	PFR
Proposed Approach (equally sized intervals)	0.82290 mol/L	CSTR (0.06756 L) + PFR (0.08030 L)
Proposed Approach (individually scaled intervals)	0.82908 mol/L	PFR (0.19515 L)
Proposed Approach (individually scaled intervals, 450 K $\leq T \leq$ 1265 K)	0.8383 mol/L	PFR (0.19498)

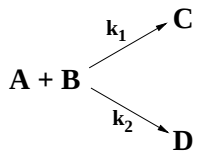

The rate expressions for these reactions are

$$r_1 = \hat{k}_1 \exp(\tfrac{-E_1}{RT}) C_A C_B^{0.3}$$
$$r_2 = \hat{k}_2 \exp(\tfrac{-E_2}{RT}) C_A^{0.5} C_B^{1.8}$$

and the kinetic parameters are given in Table 14. There are two feed streams:

- 50 L/s pure **A**, 1.0 mol/L **A**
- 50 L/s pure **B**, 1.0 mol/L **B**

The objective is to maximize the yield of **C** while minimizing the reactor volume:

$$\max 100 C_C - V_r$$

and the temperature is bounded between $450K$ and $800K$. The problem has 119 variables (17 dynamic) and 89 constraints.

Table 14: Parameters for the nonisothermal parallel reactions.

	$\hat{k}$	E	$\frac{\Delta H}{\rho C_p}$
1	5.4e7	19.138 kcal/mol	-10 K L/mol
2	3.6e5	9.569 kcal/mol	-20 K L/mol

The reactor network solution shown in Figure 23 consists of a isothermal MMR with **A** fed to the inlet of the reactor and **B** fed along the side of the reactor. In order to keep the rate of production of **D** as low as possible, the rate of reaction 2 is inhibited by keeping the concentration of **B** as low as possible. This is achieved by gradually adding **B** along the side of the reactor. The volume of the reactor is 3.3749 L, and the temperature along the reactor is held constant at the highest possible temperature (800° K). The outlet concentration of **B** is 0.48162 mol/L, and the objective value obtained is 44.787. If the objective is just the maximization of the yield of **B**, the objective value approaches the maximum possible value of 0.5 mol/L of **B** as the volume of the reactor increases. The flow rate within the reactor is shown in Figure 24. This indicates the amount of **B** that flows in through the sidestream. The concentration profiles in the reactor are shown in Figure 25.

5.2.3 Example 7—Sulfur Dioxide Oxidation

In this example, the reaction studied is the oxidation of sulfur dioxide as detailed by Lee and Aris[48]. The following equilibrium reaction is considered:

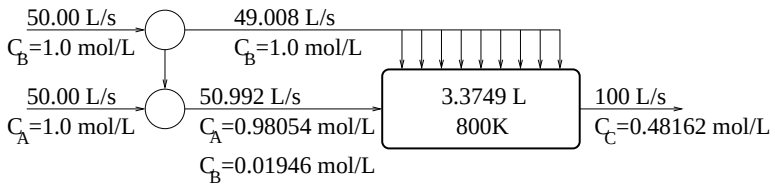

Figure 23: Reactor network solution for the nonisothermal parallel reaction.

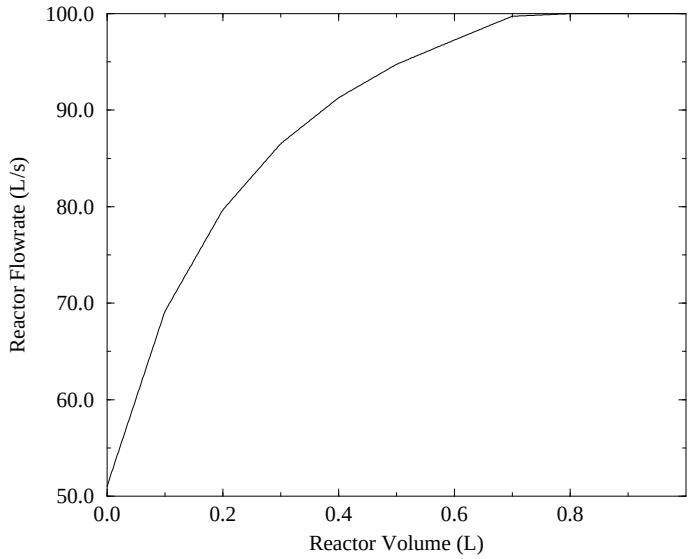

Figure 24: Flowrate profile in the MMR for the nonisothermal parallel solution.

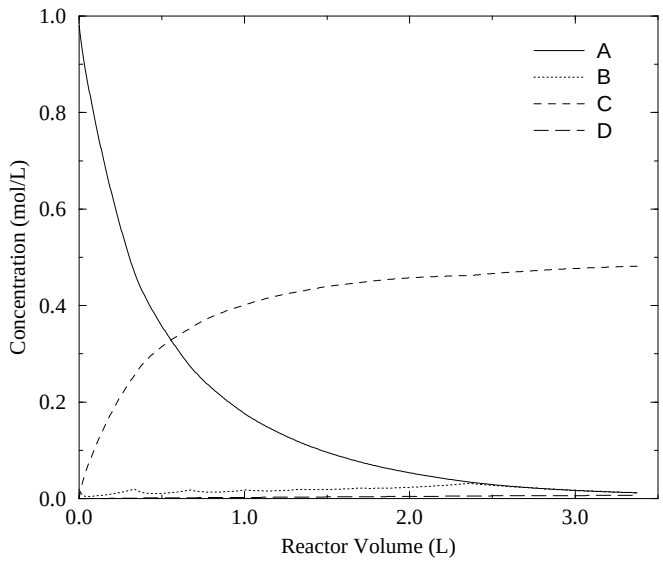

Figure 25: Concentration profiles in the MMR for the nonisothermal parallel solution.

$$\mathbf{SO_2} + \frac{\mathbf{1}}{\mathbf{2}}\mathbf{O_2} \rightleftharpoons \mathbf{SO_3}$$

The rate expression is defined as the rate of change of the extent of reaction, g per unit mass of catalyst and is given by:

$$r = k_f(p_{SO_2})^{1/2}(p_{O_2}) - k_r(p_{SO_2})^{-1/2}(p_{O_2})^{1/2}(p_{SO_3})$$

where k_f and k_r are the rate constants for the forward and reverse reactions respectively and p_i denotes the partial pressures of the species. The rate expressions for the forward and reverse reactions can be expressed in terms of the conversion and the scaled temperature t:

$$r_f = 3.6 \times 10^3 \exp\left(12.07 - \frac{50}{1+0.311t}\right) \times \left(\frac{(2.5-g)^{1/2}(3.46-0.5g)}{(32.01-0.5g)^{3/2}}\right)$$

$$r_r = 3.6 \times 10^3 \exp\left(22.75 - \frac{86.45}{1+0.311t}\right) \times \left(\frac{g(3.46-0.5g)}{(32.01-0.5g)(2.5-g)^{1/2}}\right)$$

The rates are in terms of kg mol SO_3 per kg catalyst. The feed flowrate is 7731 kg/h with a composition of 7.8 mol% SO_2, 10.8 mol% O_2, 81.4 mol% N_2.

The objective is to maximize the profit function:

$$1.15g - 0.03124\tau - 0.15t$$

where the first term indicates the revenues from the product, the second term indicates the cost of the catalyst (τ is the amount of catalyst), and the third term indicates the energy costs. Adiabatic operation of the reactors is enforced, and heat can only be added to the mixer units prior to the reactors.

The stoichiometric limit on the maximum yield of SO_3 that can be achieved is 2.5 mol SO_3 per kg of product. Using a PFR with a falling temperature profile, this limit can be approached asymptotically as larger reactors are used.

Using individual scaling, the solution as shown in Figure 26 is found to consist of a CSTR and an MMR where the sidestream is used to cool the reactor. The falling temperature profile required to increase the conversion is achieved by feeding a portion of the cold feed along the side of the reactor. The initial high temperature is achieved by first using the preheater and then reacting in a CSTR to raise the temperature further. The temperature and flowrate profiles for the MMR are shown in Figures 27 and 28. The maximum profit obtained is 2.1843.

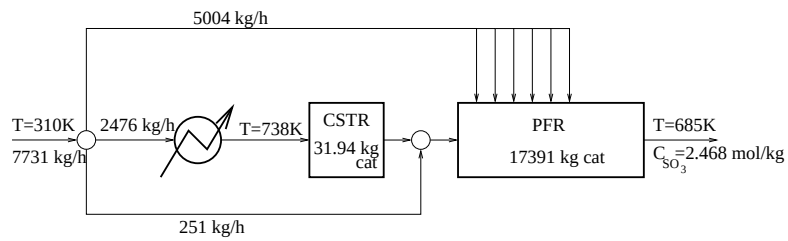

Figure 26: Reactor network solution for the sulfur dioxide reaction.

5.2.4 Example 8—Williams-Otto Process

In this example the Williams-Otto process described in Di Bella and Stevens[49] is investigated. This process consists of a reaction step followed by a separation step and involves a recycle stream. The process flowsheet is shown in Figure 30 and the three reactions and their Arrhenius parameters are shown in Table 15. The feed streams of the process are pure **A** and **B** which react to for **C**. This further reacts with **B** to form the desired product **P** along with **E**. The product is degraded by reaction with **C** to form the waste product **G**. In the separation step, the waste product **G** is decanted first, and the balance of the product is sent to a distillation column where the distillate is the product **P** and the bottoms is either purged or recycled back to the reaction step. The separation efficiency of the column is limited by the formation of an azeotrope, and the following constraints are imposed on the problem:

$$\begin{aligned} 580^\circ\text{R} \leq \quad & T \quad \leq 680^\circ\text{R} \\ 0 \text{ lb/hr} \leq \quad & F_P \quad \leq 4763 \text{ lb/hr} \end{aligned}$$

The goal is to determine the reactor network for the reaction step in the process that will maximize the return on investment. The objective function includes sales volume, raw material cost, waste treatment cost, utilities cost, expenses, a plant fixed charge, and the plant investment and is expressed as

$$\begin{aligned} J = \quad & [(8400)(0.3F_P + 0.0068F_D - 0.02F_A \\ & -0.03F_B - 0.01F_G) - 2.22F_R - 60V\rho \\ & -0.124(8400)(0.3F_P + 0.0068F_D)]/(600V\rho) \end{aligned}$$

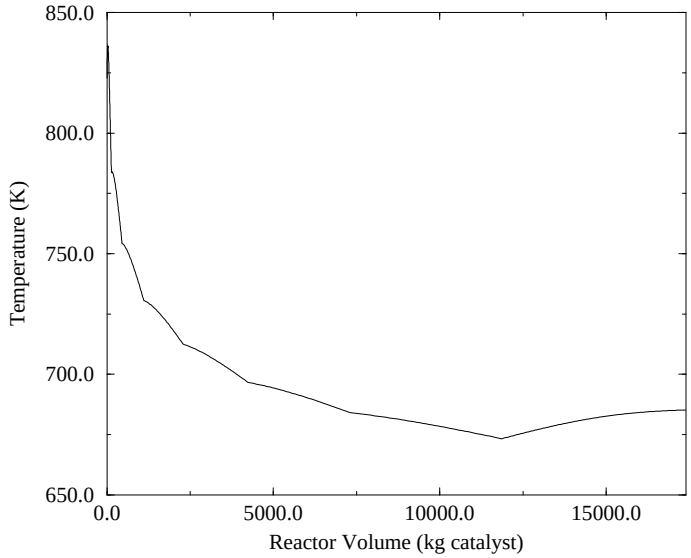

Figure 27: Temperature profile in the MMR for the sulfur dioxide solution.

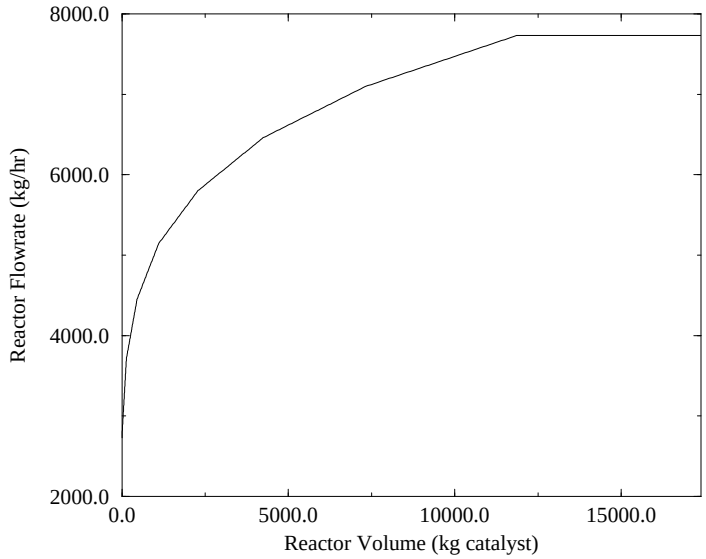

Figure 28: Flowrate profile in the MMR for the sulfur dioxide solution.

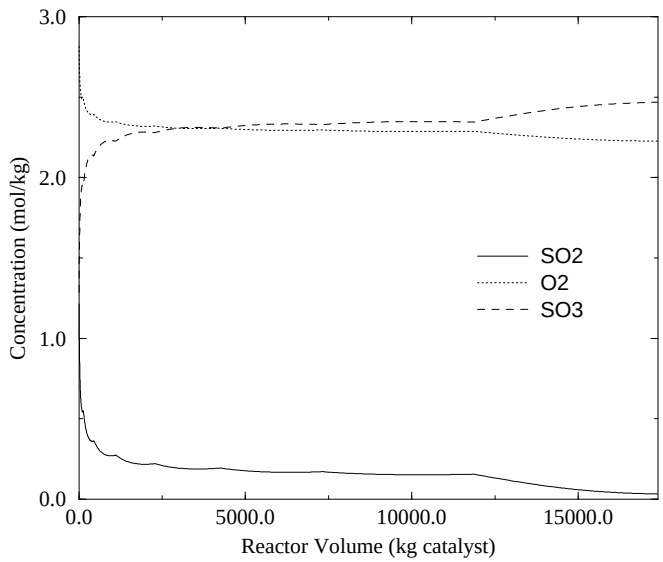

Figure 29: Concentration profile in the MMR for the sulfur dioxide solution.

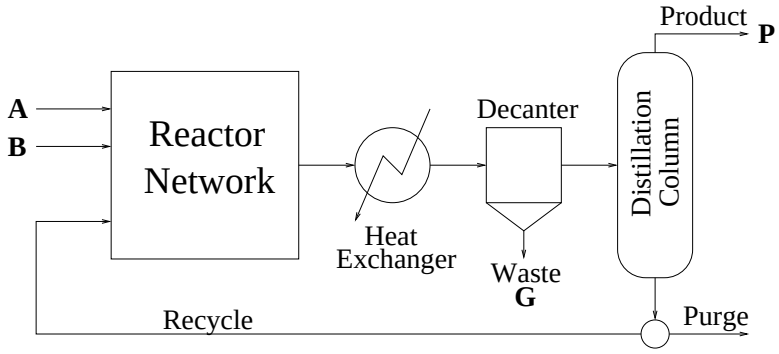

Figure 30: Flowsheet for the Williams-Otto Process.

Table 15: Reactions and parameters for the Williams-Otto Process.

Reactions	$\hat{k}$ (hr wt.frac.)$^{-1}$	E/R(°R)
$\mathbf{A+B \rightarrow C}$	$5.9755e9$	-12000
$\mathbf{C+B \rightarrow P+E}$	$2.5962e12$	-15000
$\mathbf{P+C \rightarrow G}$	$9.6283e15$	-20000

The problem has 179 variables (22 dynamic) and 138 constraints. The optimal reactor network for the problem is an isothermal PFR operating at $680°R$, and the optimal flowsheet is shown in Figure 31. The maximum return on investment is 297.83%. This is a significant improvement over the work of Di Bella and Stevens[49] which report an optimal return of 72.75%.

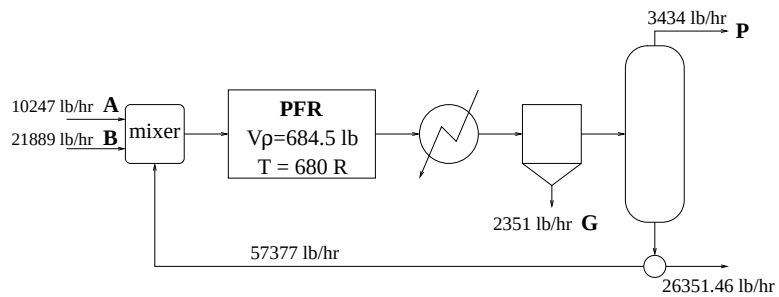

Figure 31: Optimal flowsheet for the Williams-Otto problem.

5.2.5 Example 9–Methane Conversion to Acetylene

In this example, a complex nonisothermal gas phase reaction for the conversion of methane to acetylene is considered. The mechanism involves 36 reactions and 19 species. Hydrogen is fed along with the methane feed in order to minimize to formation of carbon in the reactor.

The main products in the reaction are ethylene, acetylene, hydrogen, and benzene which leads to the formation of carbon. The objective is to maximize the production of acetylene while minimizing the production of benzene.

The kinetic constants and the reaction mechanism are taken from Olsvik et al.[50] and are shown in Table 16. The rate expression for this example is the modified Arrhenius equation:

$$k = \hat{k}T^n \exp(-E/RT)$$

This reactions take place in the gas phase and ideal gas assumptions are made. A constant pressure of 1 atm is assumed. The kinetic and thermodynamic data are obtained by MINOPT through a connection to the Chemkin package[37]. Heat capacities, enthalpies, and entropies are determined as polynomial functions of temperature. Forward rate constants are found using Arrhenius type expressions and the reverse constants are related to the forward constants through the equilibrium constants which are determined using the free energy of the reaction.

The desired mass fraction of acetylene in the product stream is 0.7 while the mass fractions of the other products are to be minimized. The objective for this problem is a weighted squares of the mass fractions in the product stream:

$$1000(y_{C_2H_2} - 0.7)^2 + 7(y_{CH_2CHCCH})^2 + 5(y_{C_4H_6})^2 + 10(y_{C_6H_6})^2$$

The problem has 518 variables (320 dynamic) and 420 constraints. The feed temperature is constrained below 1300° K.

Table 16: Mechanism and constants for the conversion of methane.

	Reaction			$\hat{k}$	n	E
1	CH_4	$\rightleftharpoons$	$CH_3 + H$	3.51×10^{15}	0.0	104000.0
2	$CH_4 + H$	$\rightleftharpoons$	$CH_3 + H_2$	1.15×10^{4}	3.0	8768.0
3	$CH_3 + CH_3$	$\rightleftharpoons$	C_2H_6	1.01×10^{15}	-0.64	0.0
4	$C_2H_6 + H$	$\rightleftharpoons$	$C_2H_5 + H_2$	5.54×10^{2}	3.5	5174.0
5	$C_2H_6 + CH_3$	$\rightleftharpoons$	$C_2H_5 + CH_4$	5.50×10^{-1}	4.0	8296.0
6	C_2H_5	$\rightleftharpoons$	$C_2H_4 + H$	2.00×10^{13}	0.0	39700.0
7	$CH_3 + CH_3$	$\rightleftharpoons$	$C_2H_4 + H_2$	1.00×10^{16}	0.0	32000.0
8	$C_2H_4 + CH_3$	$\rightleftharpoons$	$C_2H_3 + CH_4$	6.62×10^{0}	3.7	9512.0
9	$C_2H_4 + CH_3$	$\rightleftharpoons$	n-C_3H_7	2.00×10^{11}	2.53	7170.0
10	$C_2H_4 + H$	$\rightleftharpoons$	$C_2H_3 + H_2$	1.32×10^{6}	-4.783	12258.0
11	C_2H_3	$\rightleftharpoons$	$C_2H_2 + H$	1.93×10^{18}	0.0	51123.0
12	$CH_3 + C_2H_3$	$\rightleftharpoons$	C_3H_6	1.00×10^{13}	0.0	0.0
13	$n - C_3H_7$	$\rightleftharpoons$	$C_3H_6 + H$	1.58×10^{16}	0.0	38000.0
14	C_3H_6	$\rightleftharpoons$	a-$C_3H_5 + H$	1.00×10^{15}	0.0	88000.0
15	a-C_3H_5	$\rightleftharpoons$	$C_2H_2 + CH_3$	1.16×10^{10}	0.0	43200.0
16	a-C_3H_5	$\rightleftharpoons$	a-$C_3H_4 + H$	5.00×10^{13}	0.0	35000.0
17	a-$C_3H_5 + H$	$\rightleftharpoons$	a-$C_3H_4 + H_2$	1.00×10^{13}	0.0	0.0
18	$C_3H_6 + H$	$\rightleftharpoons$	a-$C_3H_5 + H_2$	5.00×10^{12}	0.0	1500.0
19	$C_2H_3 + C_2H_3$	$\rightleftharpoons$	C_4H_6	1.26×10^{13}	0.0	0.0
20	$C_2H_3 + C_2H_4$	$\rightleftharpoons$	$C_4H_6 + H$	5.00×10^{11}	0.0	7315.0
21	$C_2H_2 + H$	$\rightleftharpoons$	$C_2H + H_2$	6.02×10^{13}	0.0	22300.0
22	$C_2H_2 + CH_3$	$\rightleftharpoons$	$C_2H + CH_4$	1.81×10^{11}	0.0	17300.0
23	$C_4H_6 + H$	$\rightleftharpoons$	$C_4H_5 + H_2$	1.00×10^{14}	0.0	15000.0
24	C_4H_5	$\rightleftharpoons$	$C_4H_4 + H$	1.00×10^{14}	0.0	41400.0
25	$C_2H + H$	$\rightleftharpoons$	C_2H_2	1.81×10^{14}	0.0	0.0
26	$C_2H_3 + C_2H_2$	$\rightleftharpoons$	C_4H_5	1.10×10^{12}	0.0	4000.0
27	$CH_3 + CH_3$	$\rightleftharpoons$	$C_2H_5 + H$	1.80×10^{12}	0.0	10400.0
28	$C_4H_5 + C_2H_2$	$\rightarrow$	$C_6H_6 + H$	6.02×10^{12}	0.0	9000.0
29	C_2H_4	$\rightleftharpoons$	$C_2H_3 + H$	1.00×10^{16}	0.0	108000.0
30	$C_2H_5 + C_2H_2$	$\rightleftharpoons$	$C_2H_6 + C_2H$	2.71×10^{11}	0.0	23400.0
31	$C_2H_5 + H$	$\rightleftharpoons$	C_2H_6	3.07×10^{13}	0.0	0.0
32	C_2H_4	$\rightleftharpoons$	$C_2H_2 + H_2$	7.94×10^{12}	0.44	88760.0
33	$C_2H_3 + H$	$\rightleftharpoons$	$C_2H_2 + H_2$	9.64×10^{13}	0.0	0.0
34	$C_2H_2 + CH_3$	$\rightleftharpoons$	p-C_3H_4 + HH	6.20×10^{11}	0.0	20000.0
35	C_3H_6	$\rightleftharpoons$	p-$C_3H_4 + H_2$	8.00×10^{12}	0.44	81150.0
36	$C_3H_6 + CH_3$	$\rightleftharpoons$	a-$C_3H_5 + CH_4$	1.58×10^{12}	0.0	8800.0

The optimal solution is an MMR with hydrogen fed both to the main feed (*i.e.* cofeed with the methane) and along the side of the reactor as shown in Figure 32. The inlet temperature to the reactor is constrained to be less than 1300° K. Since high temperatures are necessary for the reaction to proceed, a rising temperature profile as shown in Figure 33 is required. The composition profiles are shown in Figure 34.

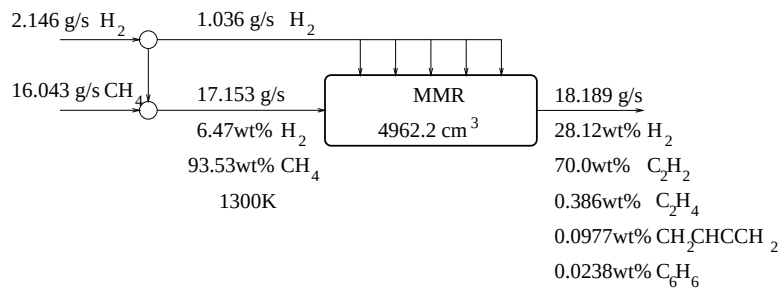

Figure 32: Reactor network solution for the methane conversion.

5.3 Local Optima

One of the most challenging aspects in optimization is guaranteeing that the global solution has been obtained. The approach proposed here relies on local nonlinear programming algorithms which only obtain the global solutions when the problem is convex. The constraints for the NLP optimization include both the time invariant algebraic constraints as well as the implicit point constraints. Due to the bilinear terms for the material balances and the exponential terms for the rate expressions, the reactor network models are nonlinear and nonconvex. In addition the implicit constraints involve the solution of a nonlinear, nonconvex set of DAEs. Although the convexity characteristics of the implicit functions can not be explicitly determined, the problem can be assumed to be highly nonconvex.

Due to the nonconvex nature of the problems, there is a possibility for multiple local solutions and thus the solutions given can not be guaranteed to be global solutions. There also is a possibility for multiple solutions with the same objective value. This may occur in the reactor network synthesis problem when redundant mixing patterns are possible in the superstructure.

Multiple local optima were found for many of the example problems by solving the problems using random starting points. (This is a feature incorporated into MINOPT.) Although all of the example problems potentially have multiple local optima, the local solutions of several problems are examined. First, for the isothermal Van de Vusse problem, Case 3, there are two local maxima in addition to the reported best solution of a CSTR (11.35 L) and PFR (16.985 L) in series which has a solution of 3.6819 mol/L. In the one local solution, a single PFR (23.637L) gives a yield of 3.57691 mol/L, and the other local solution is a single CSTR (35.599 L) is which gives a yield of 3.0607 mol/L.

For the isothermal α-pinene reaction mechanism, the best known solution is the one reported (1.557). One of the local solutions that has been reported in the literature is that of a single PFR with a volume of 6000L which gives a solution of 1.476.

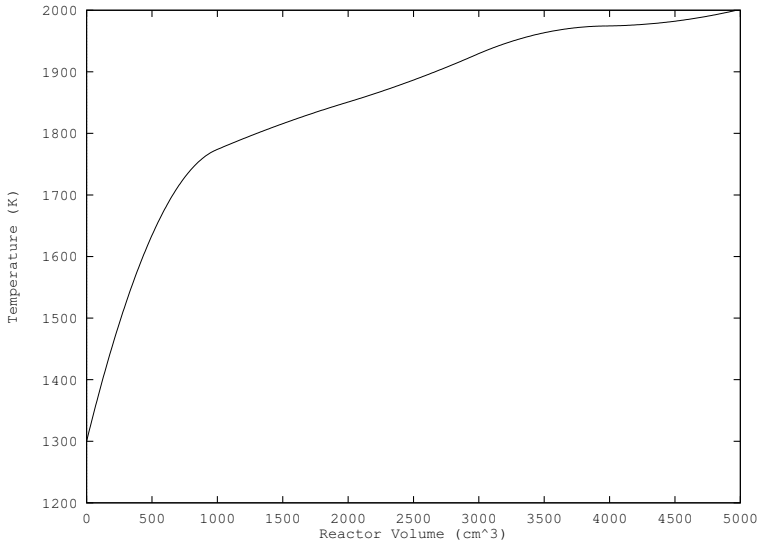

Figure 33: Temperature profile in the reactor for the methane conversion solution.

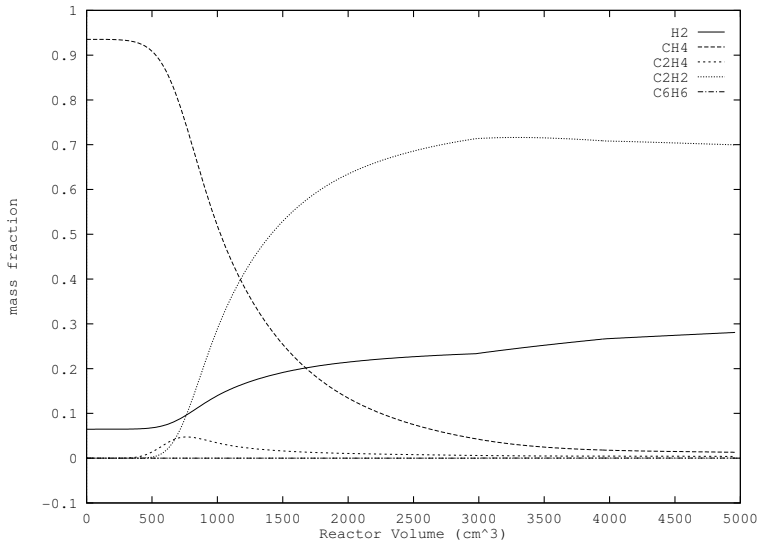

Figure 34: Composition profiles in the reactor for the methane conversion solution.

Table 17: Local solutions for the the nonisothermal Van de Vusse example—Case 2

	Optimal Yield	Solution
1	0.76750	CSTR
2	0.80893	PFR
3	0.82128	PFR
4	0.81867	PFR + CSTR
5	0.82673	PFR + CSTR
6	0.81400	CSTR + PFR

The nonisothermal Van de Vusse example, case 2, has several local optimum solutions obtained by using various starting points. The solutions obtained are listed in Table 17.

The sulfur dioxide oxidation reaction also exhibits several local optimal solutions. Besides the solution provided, there also is a trivial solution where no reaction takes place. The size of the reactors is zero, no preheating takes place, and the objective value is zero.

6 Conclusions

A new superstructure-based approach for addressing the synthesis of optimal reactor networks has been proposed. By using CSTRs and CFRs as the fundamental units in the superstructure, a sufficiently rich representation of alternatives is maintained. The differential modeling of the superstructure leads to a relatively simple problem formulation in comparison to previous superstructure based techniques. A control parameterization technique has been shown to be an effective way of solving the resulting dynamic optimization problem. By using this approach, the DAEs are integrated explicitly and no approximation is necessary.

The example problems demonstrate some of the key features of the proposed approach. The breadth of problems addressed demonstrates the generality of the overall methodology and effectiveness of the optimization strategy. The fact that improved solutions have been obtained illustrates the importance of the differential modeling as well as the effectiveness of the numerical procedure. A relatively simple superstructure including a single CFR and CSTR was able to achieve the solutions. The individual scaling of the control intervals was shown to provide improved solutions when compared to the equal scaling of the intervals. Finally, the reactor networks could be directly determined from the solution of the optimization problem.

MINOPT provides an excellent framework for modeling and solving the described problems. It allows for a succinct representation of the models and allows the user to quickly and easily change the parameters of the problem to solve a different problem.

No binary variables are required in the general formulation since the existence of a reactors and streams are determined by nonzero flowrates. However, certain situations such as fixed cost requirements for reactor existence or lower bounds for reactor existence would require binary variables for the modeling. This can be handled directly by MINOPT and such

problems should be addressed in future work.

7 Acknowledgments

The authors gratefully acknowledge financial support from the National Science Foundation and Mobil Technology Company

8 Notation

Superscripts:

a	feed stream
b	CFR side feed
c	CFR main feed
d	CSTR feed
e	CFR main exit
f	CFR side exit
g	CSTR exit
h	product
s	CFR sidestream
t	CFR internal
o	CRR side exit

Subscripts:

i	index for components set I
j	index for reactions set J
k	index for CFRs set K
l	index for CSTRs set L
r	index for feeds set R
p	index for products set P

Variables:

c	concentration [gmol/L]
C	concentration [gmol/L]
$\hat{C}_P$	molar heat capacity [J/(mol K)]
F	volumetric flowrate [L/s]
H	total molar enthalpy [J]
P	pressure [atm]
Q	energy flowrate [J/s]
r	reaction rate [mol/(L sec)]
T	temperature [K]
V	volume [L]
x	mole fraction
ρ	density [mol/L]
τ	space time [s]

Constants:

R	gas constant
k	rate constant
$\hat{k}$	Arrhenius parameter
E	Arrhenius parameter
ν	stoichiometric constants

A Constant Density Formulation

The model given in Section 2.2 is for general situations and the closure relations for the state equations are not given. The specific closure relations that should be applied vary from problem to problem. In certain cases, assumptions can be made that will simplify the closure relations and the overall model representation.

One assumption that can be applied to many problems is the constant density assumption. This assumption eliminates the need for an equation of state for the density and implies that volume is conserved. Along with the constant density assumption, the heat capacity is assumed to be the same for all the components and constant in temperature. The enthalpy is expressed as

$$\frac{dh_i}{dT} = \hat{C}$$

where $\hat{C}$ is the heat capacity.

Applying these assumptions to the general model, the following equations are obtained:

- <u>feed splitter</u>

$$F_r^a = \sum_{k \in K} F_{r,k}^{ab} + F_{r,k}^{ac} + \sum_{l \in L} F_{r,l}^{ad} \quad \forall r \in R$$

- <u>CFR sidestream mixers</u>

$$F_k^b = \sum_{r \in R} F_{r,k}^{ab} + \sum_{k' \in K} F_{k',k}^{eb} + F_{k',k}^{fb} + \sum_{l \in L} F_{l,k}^{gb} \quad \forall k \in K$$

$$c_{k,i}^b F_k^b = \sum_{r \in R} c_{r,i}^a F_{r,k}^{ab} + \sum_{k' \in K} c_{k',i}^e F_{k',k}^{eb} + c_{k',i}^f F_{k',k}^{fb} + \sum_{l \in L} c_{l,i}^g F_{l,k}^{gb} \quad \forall i \in I \quad \forall k \in K$$

$$T_k^b F_k^b = \sum_{r \in R} T_r^a F_{r,k}^{ab} + \sum_{k' \in K} T_{k'}^e F_{k',k}^{eb} + T_{k'}^f F_{k',k}^{fb} + \sum_{l \in L} T_l^g F_{l,k}^{gb} \quad \forall k \in K$$

- <u>CFR main mixers</u>

$$F_k^c = \sum_{r \in R} F_{r,k}^{ac} + \sum_{k' \in K} F_{k',k}^{ec} + F_{k',k}^{fc} + \sum_{l \in L} F_{l,k}^{gc} \quad \forall k \in K$$

$$c_{k,i}^c F_k^c = \sum_{r \in R} c_{r,i}^a F_{r,k}^{ac} + \sum_{k' \in K} c_{k',i}^e F_{k',k}^{ec} + c_{k',i}^f F_{k',k}^{fc} + \sum_{l \in L} c_{l,i}^g F_{l,k}^{gc} \quad \forall i \in I \quad \forall k \in K$$

$$T_k^c F_k^c = \sum_{r \in R} T_r^a F_{r,k}^{ac} + \sum_{k' \in K} T_{k'}^e F_{k',k}^{ec} + T_{k'}^f F_{k',k}^{fc} + \sum_{l \in L} T_l^g F_{l,k}^{gc} \quad \forall k \in K$$

- <u>CSTR feed mixers</u>

$$F_l^d = \sum_{r \in R} F_{r,l}^{ad} + \sum_{k \in K} F_{k,l}^{ed} + F_{k,l}^{fd} + \sum_{l' \in L} F_{l',l}^{gd} \quad \forall l \in L$$

$$c_{l,i}^d F_l^d = \sum_{r \in R} c_{r,i}^a F_{r,l}^{ad} + \sum_{k \in K} c_{k,i}^e F_{k,l}^{ed} + c_{k,i}^f F_{k,l}^{fd} + \sum_{l' \in L} c_{l',i}^g F_{l',l}^{gb} \quad \forall i \in I \quad \forall l \in L$$

$$T_l^d F_l^d = \sum_{r \in R} T_r^a F_{r,l}^{ad} + \sum_{k \in K} T_k^e F_{k,l}^{ed} + T_k^f F_{k,l}^{fd} + \sum_{l' \in L} T_l^g F_{l',l}^{gd} \quad \forall l \in L$$

- <u>CSTR total balance</u>

$$F_l^g = F_l^d \quad \forall l \in L$$

- <u>CSTR component balances</u>

$$F_l^g c_{l,i}^g = F_l^d c_{l,i}^d + V_l^m \sum_{j \in J} \nu_{i,j} r_{l,j}^m \quad \forall i \in I \quad \forall l \in L$$

- <u>CSTR energy balance</u>

$$\rho \hat{C} F_l^g T_l^g = \rho \hat{C} F_l^d T_l^d + V_l^m \sum_{j \in J} \Delta H_j r_{l,j}^m - Q_l^m \quad \forall l \in L$$

- <u>CSTR Reaction Rates</u>

$$r_{l,j}^m = f_{l,j}^r(c_{l,i}^m, T_l^m) \quad \forall j \in J \quad \forall l \in L$$

- <u>CFR total balance</u>

$$\frac{dF_k^t}{d\bar{V}} = -\frac{dF_k^s}{d\bar{V}} - \frac{dF_k^o}{d\bar{V}} \quad \forall k \in K$$

- <u>CFR component balance</u>

$$F_k^t \frac{dc_{k,i}^t}{d\bar{V}} = -(c_{k,i}^s - c_{k,i}^t)\frac{dF_k^s}{d\bar{V}} + V_k^t \sum_{j \in J} \nu_{i,j} r_{k,j}^t \quad \forall i \in I \quad \forall k \in K$$

- <u>CFR energy balance</u>

$$\rho \hat{C} F_k^t \frac{dT_k^t}{d\bar{V}} = -\rho \hat{C}(T_k^s - T_k^t)\frac{dF_k^s}{d\bar{V}} + \sum_{j \in J} \Delta H_j r_{k,j}^t + \frac{dQ_k^t}{d\bar{V}} \quad \forall k \in K$$

- <u>Leaving Sidestream</u>

$$F_k^o \frac{dc_{k,i}^o}{d\bar{V}} = (c_{k,i}^t - c_{k,i}^o)\frac{dF_k^o}{\bar{V}} \quad \forall i \in I \quad \forall k \in K$$

$$F_k^o \frac{dT_k^o}{\bar{V}} = (T_k^t - T_k^o)\frac{dF_k^o}{d\bar{V}} \quad \forall k \in K$$

- <u>Initial conditions ($\bar{V} = 0$)</u>

$$F_k^s = F_k^b \quad \forall k \in K$$

$$c_{k,i}^s = c_{k,i}^b \quad \forall i \in I \quad \forall k \in K$$

$$T_k^s = T_k^b \quad \forall k \in K$$

$$F_k^t = F_k^c \quad \forall k \in K$$

$$c_{k,i}^t = c_{k,i}^c \quad \forall i \in I \quad \forall k \in K$$

$$T_k^t = T_k^c \quad \forall k \in K$$

- <u>Point constraints ($\bar{V} = 1$)</u>

$$F_k^e = F_k^t \quad \forall k \in K$$

$$c_{k,i}^e = c_{k,i}^t \quad \forall i \in I \quad \forall k \in K$$

$$T_k^e = T_k^t \quad \forall k \in K$$

$$F_k^f = F_k^o \quad \forall k \in K$$

$$c_{k,i}^f = c_{k,i}^o \quad \forall i \in I \quad \forall k \in K$$

$$T_k^f = T_k^o \quad \forall k \in K$$

- <u>CFR Reaction Rates</u>

$$r^t_{k,j} = f^r_{k,j}(c^t_{k,i}, T^t_k) \quad \forall j \in J \quad \forall k \in K$$

- <u>CFR main splitters</u>

$$F^e_k = \sum_{k' \in K} F^{eb}_{k,k'} + F^{ec}_{k,k'} + \sum_{l \in L} F^{ed}_{k,l} + \sum_{p \in P} F^{eh}_{k,p} \quad \forall k \in K$$

- <u>CFR side exit splitters</u>

$$F^f_k = \sum_{k' \in K} F^{fb}_{k,k'} + F^{fc}_{k,k'} + \sum_{l \in L} F^{fd}_{k,l} + \sum_{p \in P} F^{fh}_{k,p} \quad \forall k \in K$$

- <u>CSTR product splitters</u>

$$F^g_l = \sum_{k \in K} F^{gb}_{l,k} + F^{gc}_{l,k} + \sum_{l' \in L} F^{gd}_{l,l'} + \sum_{p \in P} F^{gh}_{l,p} \quad \forall l \in L$$

- <u>product mixer</u>

$$F^h_p = \sum_{k \in K} F^{eh}_{k,p} + F^{fh}_{k,p} + \sum_{l \in L} F^{gh}_{l,p} \quad \forall p \in P$$

$$F^h_p c^h_{p,i} = \sum_{k \in K} F^{eh}_{k,p} c^e_{k,i} + F^{fh}_{k,p} c^f_{k,i} + \sum_{l \in L} F^{gh}_{l,p} c^g_{l,i} \quad \forall i \in I \quad \forall p \in P$$

$$F^h_p T^h_p = \sum_{k \in K} F^{eh} T^e_k + F^{fh} T^f_k + \sum_{l \in L} F^{gh} T^g_l \quad \forall p \in P$$

B Ideal Gas Formulation

Another assumption that is applicable to numerous problems is the ideal gas assumption. The equation of state is the ideal gas law:

$$P = \rho R T$$

The ideal gas heat capacity is given as a polynomial function of temperature:

$$\hat{C}_i = \sum_{n=1}^{N} a_{n,i} T^{n-1}$$

A convenient set of variables for this case are the total molar flowrates, N, and mole fractions, x_i.

- <u>feed splitter</u>

$$N_r^a = \sum_{k \in K} N_{r,k}^{ab} + N_{r,k}^{ac} + \sum_{l \in L} N_{r,l}^{ad} \quad \forall r \in R$$

- <u>CFR main outlet splitter</u>

$$N_k^e = \sum_{k' \in K} N_{k,k'}^{eb} + N_{k,k'}^{ec} + \sum_{l \in L} N_{k,l}^{ed} + \sum_{p \in P} N_{k,p}^{eh} \quad \forall k \in K$$

- <u>CFR side outlet splitter</u>

$$N_k^f = \sum_{k' \in K} N_{k,k'}^{fb} + N_{k,k'}^{fc} + \sum_{l \in L} N_{k,l}^{fd} + \sum_{p \in P} N_{k,p}^{fh} \quad \forall k \in K$$

- <u>CSTR outlet splitter</u>

$$N_l^g = \sum_{k \in K} N_{k,k}^{gb} + N_{k,k}^{gc} + \sum_{l' \in L} N_{l,l'}^{gd} + \sum_{p \in P} N_{l,p}^{gh} \quad \forall l \in L$$

- <u>CFR side feed mixers</u>

$$N_k^b = \sum_{r \in R} N_{r,k}^{ab} + \sum_{k' \in K} N_{k',k}^{eb} + N_{k',k}^{fb} + \sum_{l \in L} N_{l,k}^{gb} \quad \forall k \in K$$

$$x_{k,i}^b N_k^b = \sum_{r \in R} x_{r,i}^a N_{r,k}^{ab} + \sum_{k' \in K} x_{k',i}^e N_{k',k}^{eb} + x_{k',i}^f N_{k',k}^{fb} + \sum_{l \in L} x_{l,i}^g N_{l,k}^{gb} \quad \forall i \in I \quad \forall k \in K$$

$$\begin{aligned} \sum_{i \in I} h_{k,i}^b x_{k,i}^b N_k^b &= \sum_{r \in R} \sum_{i \in I} h_{r,i}^a x_r^a N_{r,k}^{ab} \\ &+ \sum_{k' \in K} \sum_{i \in I} (h_{k',i}^e x_k^e N_{k',k}^{eb} + h_{k',i}^f x_k^f N_{k',k}^{fb}) + \sum_{l \in L} \sum_{i \in I} h_{l,i}^g x_l^g N_{l,k}^{gb} \quad \forall i \in I \quad \forall k \in K \end{aligned}$$

$$h_{k,i}^b = \sum_{n=1}^{N} \frac{a_{n,i} (T_k^b)^{(n-1)}}{n} + \frac{h_i^0}{T_k^b} \quad \forall i \in I \quad \forall k \in K$$

- <u>CFR main feed mixers</u>

$$N_k^c = \sum_{r \in R} N_{r,k}^{ac} + \sum_{k' \in K} N_{k',k}^{ec} + N_{k',k}^{fc} + \sum_{l \in L} N_{l,k}^{gc} \quad \forall k \in K$$

$$x_{k,i}^c N_k^c = \sum_{r \in R} x_{r,i}^a N_{r,k}^{ac} + \sum_{k' \in K} x_{k',i}^e N_{k',k}^{ec} + x_{k',i}^f N_{k',k}^{fc} + \sum_{l \in L} x_{l,i}^g N_{l,k}^{gc} \quad \forall i \in I \quad \forall k \in K$$

$$\sum_{i\in I} h^c_{k,i} x^c_{k,i} F^c_k = \sum_{r\in R}\sum_{i\in I} h^a_{r,i} x^a_r N^{ac}_{r,k}$$
$$+ \sum_{k'\in K}\sum_{i\in I}(h^e_{k',i} x^e_k N^{ec}_{k',k} + h^f_{k',i} x^f_k N^{fc}_{k',k}) + \sum_{l\in L}\sum_{i\in I} h^g_{l,i} x^g_l N^{gc}_{l,k} \quad \forall i\in I \quad \forall k\in K$$

$$h^c_{k,i} = \sum_{n=1}^{N} \frac{a_{n,i}(T^c_k)^{(n-1)}}{n} + \frac{h^0_i}{T^c_k} \quad \forall i\in I \quad \forall k\in K$$

- <u>CSTR feed mixers</u>

$$N^d_l = \sum_{r\in R} N^{ad}_{r,l} + \sum_{k\in K} N^{ed}_{k,l} + N^{fd}_{k,l} + \sum_{l'\in L} N^{gd}_{l',l} \quad \forall l\in L$$

$$x^d_{l,i} N^d_l = \sum_{r\in R} x^a_{r,i} N^{ab}_{r,l} + \sum_{k\in K} x^e_{k,i} N^{eb}_{k,l} + x^f_{k,i} N^{fb}_{k,l} + \sum_{l'\in L} x^g_{l',i} N^{gb}_{l',l} \quad \forall i\in I \quad \forall l\in L$$

$$\sum_{i\in I} h^d_{l,i} x^b_{l,i} N^b_l = \sum_{r\in R}\sum_{i\in I} h^a_{r,i} x^a_r N^{ad}_{r,l}$$
$$+ \sum_{k'\in K}\sum_{i\in I}(h^e_{k,i} x^e_k N^{ed}_{k,l} + h^f_{k,i} x^f_k N^{fd}_{k,l}) + \sum_{l'\in L}\sum_{i\in I} h^g_{l',i} x^g_{l'} N^{gd}_{l',l} \quad \forall i\in I \quad \forall k\in K$$

$$h^d_{l,i} = \sum_{n=1}^{N} \frac{a_{n,i}(T^d_l)^{(n-1)}}{n} + \frac{h^0_i}{T^d_l} \quad \forall i\in I \quad \forall l\in L$$

- <u>Product mixers</u>

$$x^h_p N^h_p = \sum_{k\in K}(x^e_{k,i} N^{eh}_{k,p} + x^f_{k,i} N^{fh}_{k,p}) + \sum_{l\in L} x^g_{l,i} N^{gh}_{l,p} \quad \forall i\in I \quad \forall p\in P$$

$$H^h_p \rho^h_p N^h_p = \sum_{k\in K}(H^e_k \rho^e_k N^{eh}_{k,p} + H^f_k \rho^f_k N^{fh}_{k,p}) + \sum_{l\in L} H^g_l \rho^g_l N^{gh}_{l,p} \quad \forall p\in P$$

$$h^h_{p,i} = \sum_{n=1}^{N} \frac{a_{n,i}(T^h_p)^{(n-1)}}{n} + \frac{h^0_i}{T^h_p} \quad \forall i\in I \quad \forall p\in P$$

- <u>CFRs</u>

$$\frac{dN_k^t}{dV} = -\frac{N_k^s}{dV} - \frac{N_k^o}{dV} + \sum_{i\in I}\sum_{j\in J}\nu_{i,j}r_{k,j}^t \quad \forall k \in K$$

$$N_k^t\frac{dx_{k,i}^t}{dV} = (x_{k,i}^t - x_{k,i}^s)\frac{dN_k^s}{dV} + \sum_{j\in J}\nu_{i,j}r_{k,j}^t - x_{k,i}^t\sum_{i\in I}\sum_{j\in J}\nu_{i,j}r_{k,j}^t \quad \forall i \in I \quad \forall k \in K$$

$$\sum_{i\in I}(x_{k,i}^t N_k^t \hat{C}_{k,i}^t)\frac{dT_k^t}{dV} = \sum_{i\in I}(h_{k,i}^t - h_{k,i}^s)x_k^s\frac{dN_k^s}{dV} - \sum_{j\in J}h_{k,i}^o\nu_{i,j}r_{k,j}^t + \frac{dQ_k^t}{dV} \quad \forall i \in I \quad \forall k \in K$$

$$h_{k,i}^t = \sum_{n=1}^{N}\frac{a_{n,i}(T_k^t)^{(n-1)}}{n} + \frac{h_i^0}{T_k^t} \quad \forall i \in I \quad \forall k \in K$$

$$\hat{C}_{k,i}^t = \sum_{n=1}^{N}a_{n,i}(T_k^t)^{(n-1)} \quad \forall i \in I \quad \forall k \in K$$

$$x_{k,i}^t = \frac{x_{k,i}^t P}{RT_k^t}$$

- <u>side leaving streams</u>

$$N_k^o\frac{dx_{k,i}^o}{dV} = (x_{k,i}^t - x_{k,i}^o)\frac{dN_k^o}{dV} \quad \forall i \in I \quad \forall k \in K$$

$$\sum_{i\in I}(x_{k,i}^o N_k^o \hat{C}_{k,i}^o)\frac{dT_k^o}{dV} = \sum_{i\in I}(h_{k,i}^t - h_{k,i}^o)x_k^o\frac{dN_k^o}{dV} \quad \forall i \in I \quad \forall k \in K$$

$$h_{k,i}^o = \sum_{n=1}^{N}\frac{a_{n,i}(T_k^o)^{(n-1)}}{n} + \frac{h_i^0}{T_k^o} \quad \forall i \in I \quad \forall k \in K$$

$$\hat{C}_{k,i}^o = \sum_{n=1}^{N}a_{n,i}(T_k^o)^{(n-1)} \quad \forall i \in I \quad \forall k \in K$$

$$x_{k,i}^t = \frac{x_{k,i}^t P}{RT_k^o}$$

- <u>CSTRs</u>

$$x^g_{l,i}N^g_l - x^d_{l,i}N^d_l = V^m_l \sum_{j\in J} \nu_{i,j} r^m_{l,j} \quad \forall i \in I \quad \forall l \in L$$

$$N^g_l - N^d_l = \sum_{i\in I}\sum_{j\in J} \nu_{i,j} r^m_{l,j}$$

$$\sum_{i\in I} h^g_{l,i}x^g_{l,i}N^g_l - h^d_{l,i}x^d_{l,i}N^d_l = Q^m_l \quad \forall i \in I \quad \forall l \in L$$

$$x^g_{l,i} = \frac{x^g_{l,i}P}{RT} \quad \forall i \in I \quad \forall l \in L$$

$$h^g_{l,i} = \sum_{n=1}^{N} \frac{a_{n,i}(T^g_l)^{(n-1)}}{n} + \frac{h^0_i}{T^g_l} \quad \forall i \in I \quad \forall l \in L$$

References

(1) Floudas, C. A. *Nonlinear and Mixed Integer Optimization: Fundamentals and Applications*; Oxford University Press, 1995.

(2) Hildebrandt, D.; Biegler, L. T. Synthesis of Reactor Networks. In *Foundations of Computer Aided Process Design*; Biegler, L. T.; Doherty, M. F., Eds.; vol. 91 of *AIChE Symposium Series* AIChE New York 1995 52.

(3) Dyson, D. C.; Horn, F. J. M. Optimum Adiabatic Cascade Reactor with Direct Intercooling. *J. Opt. Theory Applic.* **1967**, *1* (1), 40.

(4) Horn, F. J. M.; Tsai, M. J. The Use of Adjoint Variablesin the Development of Improvement Criteria for Chemical Reactors. *J. Opt. Theory Applic.* **1967**, *1* (2), 131.

(5) Jackson, R. Optimization of Chemical Reactors with Respect To Flow Configuration. *J. Opt. Theory Applic.* **1968**, *2*, 240.

(6) Ravimohan, A. L. Optimization of Chemical Reactor Networks. *J. Opt. Theory Applic.* **1971**, *8*, 204.

(7) Paynter, J. D.; Haskins, D. E. Determination of Optimal Reactor Type. *Chem. Eng. Sci* **1970**, *25*, 1415.

(8) Achenie, L. K. E.; Biegler, L. T. Algorithmic Synthesis of Chemical Reactor Networks Using Mathematical Programming. *Ind. Eng. Chem. Fund.* **1986**, *25*, 621.

(9) Achenie, L. K. E.; Biegler, L. T. A Superstructure Based Approach to Chemical Reactor Network Synthesis. *Comput. Chem. Eng.* **1990**, *14* (1), 23.

(10) Kokossis, A. C.; Floudas, C. A. Optimization of Complex Reactor Networks—I. Isothermal Operation. *Chem. Eng. Sci.* **1990**, *45* (3), 595.

(11) Kokossis, A. C.; Floudas, C. A. Synthesis of Isothermal Reactor-Separator-Recycle Systems. *Chem. End. Sci.* **1991**, *46* (5/6), 1361.

(12) Kokossis, A. C.; Floudas, C. A. Optimization of Complex Reactor Networks—II. Nonisothermal Operation. *Chem. Eng. Sci.* **1994**, *49* (7), 1037.

(13) Kokossis, A. C.; Floudas, C. A. Stability in Optimal Design: Synthesis of Complex Reactor Networks. *AIChE J.* **1994**, *40* (5), 849.

(14) Horn, F. Attainable Regions in Chemical Reaction Technique. In *The Third European Symposium on Chemical Reaction Engineering* Pergamon, 1964 1–10.

(15) Glasser, D.; Crowe, C.; Hildebrandt, D. The Attainable Region and Optimization in Concentration Spaces. *Ind. Eng. Chem. Res* **1987**, *26* (9), 1803.

(16) Hildebrandt, D.; Glasser, D.; Crowe, C. M. Geometry of the Attainable Region Generated by by Reaction and Mixing: with and without Constraints. *Ind. End. Chem. Res.* **1990**, *29*, 49.

(17) Hildebrandt, D.; Glasser, D. The Attainable Region and Optimal Reactor Structures. *Chem. Eng. Sci.* **1990**, *45*, 2161.

(18) Achenie, L. K. E.; Biegler, L. T. Developing Targets for the Performance Index of a Chemical Reactor Network. *Ind. Eng. Chem. Res.* **1988**, *27*, 1811.

(19) Balakrishna, S.; Biegler, L. T. A Constructive Targeting Approach for for the Synthesis of Isothermal Reactor Networks. *Ind. Eng. Chem. Res.* **1992**, *31* (9), 300.

(20) Balakrishna, S.; Biegler, L. T. Targeting Strategies for Synthesis and Energy Integration of Nonisothermal Reactor Networks. *Ind. Eng. Chem. Res.* **1992**, *31* (9), 2152.

(21) Balakrishna, S.; Biegler, L. T. Chemical Reactor Network Targeting and Integration: An Optimization Approach. In *Advances in Chemical Engineering*; Anderson, J. L., Ed.; vol. 23 Academic Press, 1996, p 247–300.

(22) Lakshmanan, A.; Biegler, L. T. Synthesis of Optimal Chemical Reactor Networks. *Ind. Eng. Chem. Res.* **1996**, *35* (4), 1344.

(23) Feinberg, M.; Hildebrandt, D. Optimal Reactor Design from a Geometric Viewpoint—I. Universal Properties of the Attainable Region. *Chem. Eng. Sci.* **1997**, *52* (10), 1637.

(24) Bryson, A. E.; Ho, Y.-C. *Applied Optimal Control*; Hemisphere Publishing Corporation: Washington, 1988.

(25) Luus, R. Optimal Control by Dynamic Programming Using Systematic Reduction in Grid Size. *Int. J. Control* **1990**, *5*, 995.

(26) Luus, R. Application of Dynamic Programming to High-Dimensional Non-Linear Optimal Control Problems. *Int. J. Control* **1990**, *52*, 239.

(27) Luus, R.; Rosen, O. Application of Dynamic Programming to Final State Constrained Optimal Control Problems. *Ind. Eng. Chem. Res.* **1991**, *30*, 1525.

(28) Luus, R. Piecewise Linear Continuous Optimal Control by Iterative Dynamic Programming. *Ind. Eng. Chem. Res.* **1993**, *32*, 859.

(29) Cuthrell, J. E.; Biegler, L. T. On the Optimization of Differential-Algebraic Process Systems. *AIChE J.* **1987**, *33*, 1257.

(30) Logsdon, J. S.; Biegler, L. T. Accurate Solution of Differential-Algebraic Optimization Problems. *Ind. Eng. Chem. Res.* **1989**, *28*, 1628.

(31) Vasantharajan, S.; Biegler, L. T. Simultaneous Strategies for Optimization of Differential-Algebraic Systems with Enforcement of Error Criteria. *Comput. Chem. Eng.* **1990**, *14*, 1083.

(32) Vassiliadis, V. S.; Sargent, R. W. H.; Pantelides, C. C. Solution of a Class of Multistage Dynamic Optimization Problems. 1. Problems without Path Constraints. *Ind. Eng. Chem. Res.* **1994**, *33*, 2111.

(33) Vassiliadis, V. S.; Sargent, R. W. H.; Pantelides, C. C. Solution of a Class of Multistage Dynamic Optimization Problems. 2. Problems with Path Constraints. *Ind. Eng. Chem. Res.* **1994**, *33*, 2123.

(34) Schweiger, C. A.; Floudas, C. A. Interaction of Design and Control: Optimization with Dynamic Models. In *Optimal Control: Theory, Algorithms, and Applications*; Hager, W. W.; Pardalos, P. M., Eds.; Kluwer Academic Publishers, 1997, p 388–435.

(35) Schweiger, C. A.; Floudas, C. A. *MINOPT: A Software Package for Mixed-Integer Nonlinear Optimization*; Princeton University Princeton, NJ 08544-5263 1997 Version 2.0.

(36) Schweiger, C. A.; Floudas, C. A. *MINOPT A Modeling Language and Algorithmic Framework for Linear, Mixed-Integer, Nonlinear, Dynamic, and Mixed-Integer Nonlinear Optimization*; Kluwer Academic Publishers, 1998 in preparation.

(37) Kee, R. J.; Rupley, F. M.; Meeks, E.; Miller, J. A. *Chemkin-III: A FORTRAN Chemical Kinetics Package for the Analysis of Gas-Phase Chemical and Plasma Kinetics*; Sandia National Laboratories Livermore, CA 1996.

(38) CPLEX Optimization, Inc. *Using the CPLEX Callable Library*; CPLEX Optimization, Inc. 1995.

(39) Murtagh, B. A.; Saunders, M. A. *MINOS 5.4 User's Guide*; Systems Optimization Laboratory Department of Operations Research, Stanford University 1993 Technical Report SOL 83-20R.

(40) Gill, P. E.; Hammarling, S. J.; Murray, W.; Saunders, M. A.; Wright, M. H. *User's Guide for LSSOL (Version 1.0): A Fortran Package for Constrained Linear Least-Squares and Convex Quadratic Programming*; Systems Optimization Laboratory Department of Operations Research, Stanford University 1986.

(41) Gill, P. E.; Murray, W.; Saunders, M.; Wright, M. H. *User's Guide for NPSOL (Version 4.0)*; Systems Optimization Laboratory Department of Operations Research, Stanford University 1986 Technical Report SOL 86-2.

(42) Gill, P. E.; Murray, W.; Saunders, M. A. *User's Guide for SNOPT 5.0: A Fortran Package for Large-Scale Nonlinear Programming*; Systems Optimization Laboratory Department of Operations Research, Stanford University 1997.

(43) Jarvis, R. B.; Pantelides, C. C. *DASOLV: A Differential-Algebraic Equation Solver*; Center for Process Systems Engineering Imperial College of Science, Technology, and Medicine, London 1992 Version 1.2.

(44) Brenan, K. E.; Campbell, S. L.; Petzold, L. R. *Numerical Solution of Initial-Value Problems in Differential-Algebraic Equations*; SIAM, 1996.

(45) Chitra, S. P.; Govind, R. Yield Optimization for Complex Reactor Systems. *Chem. Eng. Sci.* **1981**, *36*, 1219.

(46) Chitra, S. P.; Govind, R. Synthesis of Optimal Serial Reactor Structures for Homogeneous Reactions. *AIChE J.* **1985**, *31* , 185.

(47) Levenspiel, O. *The Chemical Reactor Omnibook*; OSU Book Stores, Inc, 1993.

(48) Lee, K.; Aris, R. Optimal Adiabatic Bed Reactors for Sulfur Dioxide with Cold Shot Cooling. *Ind. Eng. Chem. Proc. Des. Dev.* **1963**, *2* (4), 300.

(49) Di Bella, C. W.; Stevens, W. F. Process Optimization by Nonlinear Programming. *Ind. Eng. Chem. Proc. Dev. Des.* **1965**, *4* (1), 16.

(50) Olsvik, O.; Rokstad, O. A.; Holmen, A. Pyrolysis of Methane in the Presense of Hydrogen. *Chem. Eng. Technol.* **1995**, *18*, 349.